ABSTRACT

Murray, Gary Christopher. Dissolution of phosphate in mixed Fe- and Al-oxide mineral suspensions as influenced by reducing conditions. (Under the direction of D.L. Hesterberg)

The loss of soil phosphorus (P) to surface waters poses a threat to water quality. Research evaluating P dissolution and transfer among sorbents in pure mineral systems can provide basic knowledge useful for the environmental management of P. The objective of this research was to evaluate the effect of Al-oxides on the reductive dissolution of orthophosphate sorbed to Fe-oxides. Redox reactor systems containing 0.5 g ferrihydrite [$Fe(OH)_3$] kg^{-1} suspension and 0.002 to 0.7 g boehmite (α-AlOOH) kg^{-1} suspension were equilibrated with 750 mmol P kg^{-1} of ferrihydrite, and abiotically reduced for 72 h with 0.5% $H_{2\,(g)}$ in the presence of a catalyst of 10 % Pt on activated C. The kinetics of reductive dissolution of ferrihydrite, as indicated by dissolved Fe(II), followed a linear (zero-order) model. The rate coefficient showed a sharp, linear decrease ($R^2 = 0.61$) with minor additions of boehmite (0 to 0.008 g kg^{-1}), and net Fe(II) dissolution was essentially null for boehmite additions $\geq$ 0.02 g. Uptake of dissolved P occurred over time during reduction of mixed ferrihydrite-boehmite suspensions. XANES spectroscopy of samples collected during reduction of a 1:1 ferrihydrite: boehmite mixture did not detect a net transfer of P from ferrihydrite to boehmite over 168 h. Supporting experiments suggested that Al(III) dissolved from poorly crystalline boehmite caused the observed decrease in Fe(II) dissolution rate in the reduction reactors, either by sorbing to the ferrihydrite surface and blocking electron transfer, or by sorbing to Pt/C catalyst and inhibiting its catalytic activity. The results suggest that Al-oxides may affect net phosphate dissolution in soils undergoing reduction by taking up dissolved P or by

inhibiting the reductive dissolution of iron oxides if Al(III) is sorbed to Fe(III)-oxide surfaces.

DISSOLUTION OF PHOSPHATE IN MIXED FE- AND AL-OXIDE MINERAL SUSPENSIONS AS INFLUENCED BY REDUCING CONDITIONS

By

Chris Murray

A thesis submitted to the Graduate Faculty of
North Carolina State University
in partial fulfillment of
the requirements for the Degree
of Master of Science

SOIL SCIENCE

Raleigh

2004

APPROVED BY:

_____ _____

_____
Chair of Advisory Committee

BIOGRAPHY

Gary Christopher Murray was born and raised on a small farm in Snow Camp, North Carolina to Gary and Wanda Murray. The author attended Southern Alamance High School, where he began to develop an interest in the field of agriculture. The author began his B.S. in Agronomy in the Fall of 1998. While an undergraduate at N.C. State, the author was active in Campus Crusade for Christ, where he met the love of his life, Ms. Jamie Brie Wiley.

The author completed his B.S. in Agronomy with a minor in Environmental Sciences in the Spring of 2002, and began graduate study the next fall under the direction of Dr. Dean Hesterberg. The author was married to Jamie Brie Wiley in October, 2002.

Eston Christopher Murray was born to the author and Jamie Brie in September 2004. The author has accepted a job with an environmental consulting firm in Raleigh, NC, and is quite excited about utilizing his knowledge of soil chemistry in the professional world.

ACKNOWLEDGEMENTS

There have been many individuals whose encouragement and support were invaluable for the completion of this degree. I would like to acknowledge some of them here. I have enjoyed the friendship of Ryan Harrelson and Chris Brownfield, fellow graduate students and office mates. Kim Hutchison has been a tremendous source of help in the laboratory, as well as a good friend. I am grateful for the input of my graduate committee members Drs. Phillip Westerman and Michael Vepraskas, and for the guidance, patience and friendship of my advisor, Dr. Dean Hesterberg.

I want to thank my family, both the Murray's and the Wiley's. They have strengthened and encouraged me many times when I felt like giving up. I hope I have made all of you proud, as I know I couldn't have done it without you.

I am grateful for my son Eston. He came into the world exactly when he was supposed to, and gave things the perspective that they needed. I love you son, and I pray that this degree has helped to make me a stronger father and provider for you.

Most importantly, I want to thank my wife Jamie Brie Murray. Your patience and sacrifice have been tremendous. This degree was much more endurable thanks to your companionship. I love you now and always.

TABLE OF CONTENTS

LIST OF TABLES

LIST OF FIGURES

LIST OF APPENDIX FIGURES

Chapter One: General Introduction

CHAPTER ONE – GENERAL INTRODUCTION

Environmental Impacts of Phosphorus

Phosphorus (P) is an essential macronutrient for biological growth and development. It serves as a structural element in cells and is a vital component of energy metabolism via adenosine triphosphate (ATP) (Rausch and Bucher, 2002). Extensive research has been conducted to elucidate mechanisms of both plant availability and sorption of soil P (Wild, 1950, Holford and Patrick, 1978, White, 1982, Mengel, 1985, Anghinoni et. al., 1996). While much work has been undertaken to understand soil P dynamics, many gaps in our knowledge of this nutrient still exist, particularly with respect to mobility in phosphorus-enriched soils.

Application of animal wastes to agronomic soils often provides an effective means for waste disposal while providing plant nutrients. Historically, animal wastes were applied based on the plant-available nitrogen content (Eghball and Power, 1999). Since the P content of animal wastes is often greater than the nitrogen content, accumulation of soil phosphorus at levels exceeding agronomic utilization of P has resulted (Mikkelsen, 1997, Correl, 1998). This buildup of soil P has increased the potential for P mobilization and discharge into waterways.

Because phosphorus is a limiting nutrient in aquatic systems, it can cause prolific algal growth when transported to surface waters via soil solution or surface runoff (Sharpley et al., 1993, Pant and Reddy, 2001). This enhanced algal growth, known as eutrophication, is the source of much environmental concern. As a result of the concerns arising from eutrophication, the USDA-NRCS has implemented a policy to limit the application of animal wastes to soils that contain elevated levels of soil P (NRCS 590

Standard, 1999). These application limits can have significant impacts on productivity and profitability of U.S. animal agriculture. A detailed understanding of fundamental soil phosphorus chemistry is therefore needed to develop sound management practices that allow more precise regulation of soil P and minimize impacts on water quality.

Phosphorus – Soil Interactions

Elucidation of soil phosphorus transport mechanisms is necessary to accurately predict the environmental fate of this nutrient. The soil phosphorus model in Figure 1.1 illustrates some potential fates of soil P. Anthropogenic influences such as the application of animal wastes have a pronounced effect on the amount of P entering the soil. Portions of applied P have the potential to enter surface waters directly as sediment discharged to streams from soil erosion, or as dissolved P. The remaining P is sorbed in the soil matrix, or bound in the source solids. A soluble soil P pool will also be present.

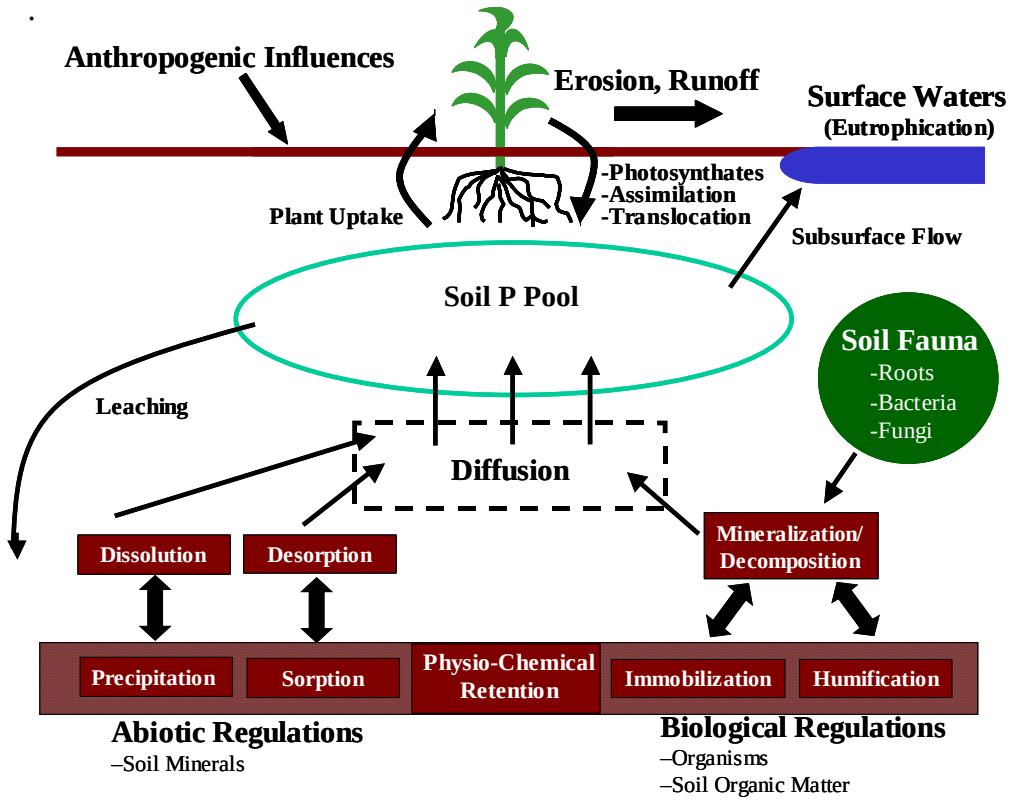

Figure 1.1. The soil phosphorus cycle (Adapted from Frossard et al, 1995).

Plants may contribute to or deplete this pool by providing photosynthates and decomposition products, or by taking up portions of this soluble P (Frossard et al., 1995).

Other soil processes contribute to this soluble P pool. Native microbial populations have the ability to contribute to dissolved P by mineralizing organic phosphorus (Cosgrove, 1977). Immobilization may also occur when soil microbes convert dissolved P to organic forms (Cole et al., 1977, Hughes and Renolds, 1991).

Soil parent materials containing P-rich primary and secondary minerals may undergo dissolution, subsequently contributing to soil solution P (Lindsay et al., 1989). This dissolution may be enhanced at both high and low pH (Lindsay, 1979). Desorption from soil mineral surfaces may also contribute to the soil P pool, particularly when the contact time between the mineral and adsorbed P is short (Barrow, 1979, Torrent et al., 1992).

The dissolved P pool may contain various forms of phosphate. While the orthophosphate ion is expected to predominate, soluble organic phosphorus or aqueous complexes of Fe, Al and Ca-phosphates may also be present (Frossard et al., 1995, Dolfing et al., 1999). The soluble phosphorus pool is of environmental concern because of its mobility and potential to contaminate surface waters. Research has shown that soluble phosphate may leach when P enriched soils are artificially drained and have reached a threshold P sorption capacity (Heckrath et al., 1995, Sims et al., 1998). Subsurface flow of soluble P has also been documented as a viable point of loss to surface waters (Sims et al., 1998, Kleinman et al., 2003).

The sorbed phase of phosphorus is of particular interest in environmental phosphorus research since this portion is responsible for a tremendous amount of P

retention in soils. Phosphate in this phase can be bound to clay minerals such as kaolinite (Schwertmann and Herbillon, 1992), or other secondary soil minerals such as iron and aluminum oxides (D. Freese et al., 1992). Iron and aluminum oxides are generally considered the most important sorbents of P in soils (van der Zee and van Riemsdijk, 1986).

Reductive Dissolution of Soil Phosphate

Iron oxides are found in soils from a variety of climatic regions, and are considered the most abundant metallic oxides in soils (Schwertmann and Taylor, 1989). These minerals form from oxidation of ferrous iron released during primary mineral weathering (Birkeland, 1974, Schwertmann and Taylor, 1989). Aluminum oxides are found in soils as a result of the weathering of minerals such as kaolinite or silica (Buol et al., 1997). These secondary minerals are responsible for a tremendous amount of chemical reactivity and nutrient retention in acidic soils, and are responsible for the majority of total soil P sorption capacity (van der Zee and van Riemsdijk, 1988, Pena and Torrent, 1990, D. Freese et al., 1992).

Beauchemin and Simard (1999) reviewed various phosphorus saturation indices utilized throughout the world. Of the sixteen indices cited, ten utilized measurements related to iron and aluminum oxide content as a means of determining P saturation (Beauchemin and Simard, 1999). As iron oxide minerals dissolve during reduction and are subsequently reprecipitated, increases in mineral surface area and P sorption capacity are expected (Patrick and Khalid, 1974, Vadas and Sims, 1999). Greater P retention is also associated with amorphous Al minerals (Pierzynski et al., 1990, D. Freese et al., 1992, Darke and Walbridge, 2000). Phosphate sorption in soils can then be accurately

predicted based on the poorly-crystalline iron and aluminum content (Beauchemin and Simard, 1999, Vadas and Sims, 1999).

The phenomenon known as reductive dissolution has been well documented in soil phosphorus research (Patrick et al., 1973, Holford and Patrick, 1979, DeLaune et al., 1981, Husin et al., 1987, Moore and Reddy, 1994, Sallade and Sims, 1997). This process involves the dissolution of P under reducing conditions, presumably due to reductive dissolution of Fe(III) with which the P is associated. This hypothesis is based on correlations between iron and phosphorus in solution found under reducing conditions (Patrick et al., 1973, Sallade and Sims, 1997, Vadas and Sims, 1998). Figure 1.2 illustrates a concept of this process for adsorbed PO_4^{-3}. Iron(III) in oxide minerals may undergo reduction to iron(II) under reducing soil conditions. In iron oxide minerals,

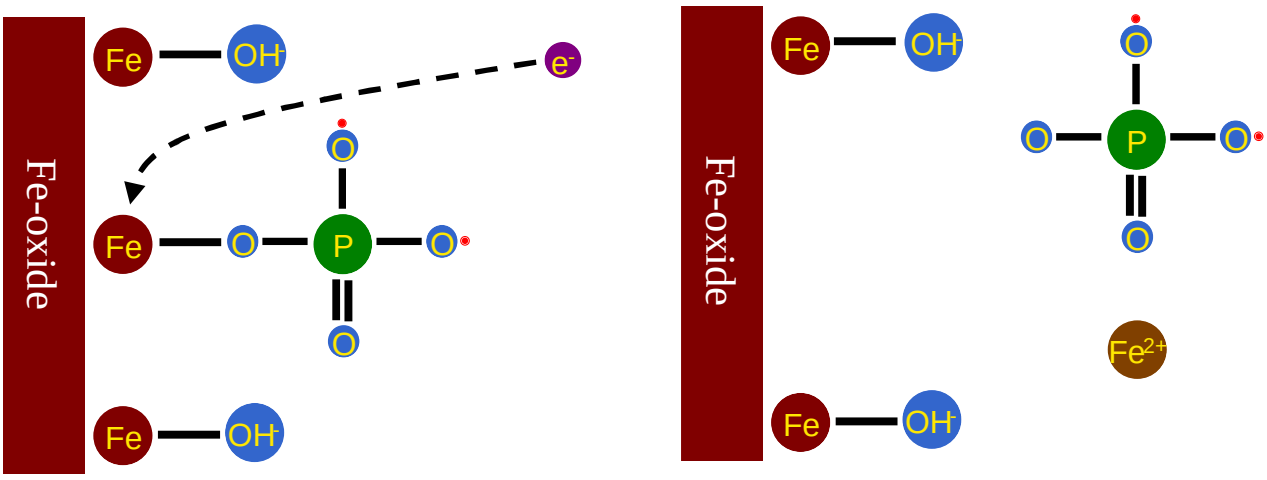

Figure 1.2. Schematic representation of the reductive dissolution mechanism for soil P. Redrawn from Hesterberg, 2004.

these changes result in a net dissolution of the mineral surface and a subsequent release of ferrous iron. Phosphate associated with the surface of these minerals may therefore be

released during this dissolution process, potentially resulting in a net dissolution of phosphate.

There are several environmental scenarios where reductive dissolution could be linked to excessive P dissolution. Iron oxides are expected to be reductively dissolved at Eh values of 100 mV or less in soils at circumneutral pH (Ponnamperuma, 1972). Whenever such conditions are met, phosphate associated with iron oxides also has the potential to dissolve.

Soils that are wet or poorly drained will periodically develop low (< 100 mV) soil redox potential when saturation occurs and microbes are decomposing organic matter. As they oxidize organic matter, microbes reduce a variety of terminal electron acceptors in the order of O_2, NO_3^-, MnO_2 (Mn(IV)-oxides), $Fe(OH)_3$ (Fe(III)-oxides), SO_4^{2-}, and CO_2 (Bartlett and James, 1993). Reductive P dissolution is expected if Eh values remain at or below levels sufficient to cause iron oxide reduction. Wet or poorly drained soils are found in a variety of environmental settings. Constructed or converted wetlands with excess levels of sorbed P would experience conditions sufficient to allow Fe-oxide reduction (Pant et al., 2002). Similarly, reductive P dissolution may occur in naturally occurring wetlands. Phosphorus laden sediments deposited along streams or riverbanks and drainage ditches could experience similar reductive dissolution processes (Sallade and Sims, 1997, Koski-Vahala and Hartikainen, 2001).

While the soil P chemistry literature provides evidence for reductive P dissolution, studies that investigate the process at the fundamental level are lacking. For example, many reductive dissolution studies are conducted on soils, and reduction is accomplished through native microbial populations utilizing Fe(III) as an electron

acceptor under reducing conditions (Moore and Reddy, 1994, Sallade and Sims, 1997). Organic matter found in these soils may complicate the effects of reductive P dissolution by enhancing the P sorption ability of the mineral surface (Borggaard et. al., 1990), or through the formation of aqueous (or solid phase) ternary complexes involving organic matter, Fe, Al and phosphate (Gerke and Herman, 1992). Reductive dissolution studies in pure mineral systems may help elucidate Fe- and Al-oxide interactions with P during reduction, and expose the role of Al-oxides as a non redox-active sink for reductively dissolved P.

Application of Reductive Dissolution Research

In response to the P regulation requirements of the Natural Resources Conservation Service Revised Nutrient Management (590) Field Office Technical Guide Standard of 1999 (NRCS 590 Standard, 1999), a technical tool was developed in the state of North Carolina. The Phosphorus Loss Assessment Tool (PLAT) is a computerized P management device developed by a team of soil scientists, engineers and practitioners at North Carolina State University, the North Carolina Department of Environment and Natural Resources, the North Carolina Department of Agriculture and the USDA Natural Resources Conservation Service. This tool rates an agricultural field for potential P loss to surface waters. The PLAT considers 1) runoff or surface P loss, 2) P loss from leaching, 3) P source effects on P loss and 4) sediment or particulate P loss (PLAT, 2004). Each of these components is used to provide an overall rating for a given agricultural field. Because of the regulatory nature of the PLAT, soils receiving very high P loss potential ratings will be prohibited from having P applied.

While extensive research has been conducted to develop this P loss model, additional research investigating the basic chemistry behind reductive P dissolution may provide a more accurate rating from the sediment (particulate) P loss component, particularly for P laden eroded particles deposited as sediment in a reducing environment such as a ditch or stream. Currently, the total erosion rate, the total P sorbed on eroded particles, P delivery ratios of various BMP's and Fe-bound P are taken into consideration for this component of the PLAT. The model considers Fe-bound P to be available, since this constituent has the potential to dissolve under anaerobic conditions and release P into solution. That proportion of P associated with aluminum in minerals (Al-bound P) is then considered unavailable. Additionally, the portion of soil P dissolved under reducing conditions in agricultural soils (i.e., controlled drainage) also needs further consideration. Further research into the specific interactions between Fe-oxides, Al-oxides and P during reduction may provide further insight for the particulate and dissolved P loss components. Evaluation of the role of Al-oxides as a sorbent for P released from Fe-oxides under reducing conditions may generate more sound ratings from this portion of the PLAT.

The goal of this research was to explore the basic chemistry behind the reductive dissolution of phosphate associated with Fe-oxide minerals in systems with mixtures of Fe- and Al-oxides. Mixtures of poorly crystalline Fe- and Al-oxides were abiotically reduced for up to 72 hours, and dissolved Fe, PO_4, and other chemical parameters were evaluated over time.

The specific objectives of the study were to determine the rate of reductive dissolution of ferrihydrite [synthetic ferric hydroxide - $Fe(OH)_3$] and dissolution of

phosphate during abiotic reduction as affected by the amount of added boehmite (α-AlOOH) in aqueous ferrihydrite/boehmite mixtures, and to determine some possible mechanisms for any changes in net reductive dissolution of P as affected by boehmite.

REFERENCES CITED

Anghinoni, I., Baligar, V.C., and R.J. Wright. 1996. Phosphorus sorption isotherm characteristics and availability parameters of Appalachian acidic soils. Commun. Soil Sci. Plant Anal. 27:2033-2048.

Barrow, N.J. 1979. The description of desorption of phosphate from soil. J. of Soil Sci., 30:259-270.

Bartlett, R.J. and B.R. James. 1993. Redox chemistry of soils. Adv. Agron. 50:151-208.

Beauchemin, S. and R.R. Simard. 1999. Soil phosphorus saturation degree: Review of some indices and their suitability for P management in Quebec, Canada. Can. J. Soil Sci. 79:615-625.

Birkeland, P.W. 1974. Pedology, weathering and geomorphological research. Oxford University Press. New York, NY.

Borggaard, O.K., Jorgensen, S.S., Moberg, J.P., and B. Raben-Lange. 1990. Influence of organic matter on phosphate adsorption by aluminum and iron oxides in sandy soils. J. Soil Sci. 41:443-449.

Buol, S.W., Hole, F.D., McCracken, R.J., and R.J. Southard. 1997. Soil Genesis and Classification. Iowa State University Press., Ames IA.

Cole, C.V., Innis, G.S., and J.W.B. Stewart. 1977. Simulation of phosphorus cycling in semiarid grasslands. Ecology. 58:1-15.

Correll, D.L. 1998. The role of phosphorus in the eutrophication of receiving waters: A review. J. Environ. Qual. 27:261-266.

Cosgrove, D.J., 1977. Microbial transformations in the phosphorus cycle. Adv. Microbial Ecol. 1:95-134.

Darke, A.K., and M.R. Walbridge. 2000. Al and Fe biogeochemistry in a floodplain forest: Implications for P retention. Biogeochemistry. 51:(1) 1-32.

DeLaune, R.D., Reddy, C.N. and W.H. Patrick, Jr. 1981. Effect of pH and redox potential on concentration of dissolved nutrients in estuarine sediment. J. Environ. Qual. 10:276-279.

Dolfing, J., Chardon, W. J., and J. Japenga. 1999. Association between colloidal iron, aluminum, phosphorus, and humic acids. Soil Sci. 164(3): 171-179.

Eghball, B., and J.F. Power. 1999. Phosphorus- and Nitrogen-based manure and compost applications: Corn production and soil phosphorus. Soil Sci. Soc. Am. J. 63:895-901.

Freese, D., S.E.A.T.M. Van der Zee, and W.H. Van Riemsdijk. 1992. Comparison of different models for phophate sorption as a function of the iron and aluminum oxides of soils. J. Soil Sci. 43:729-738.

Frossard, E., Brossard, M., Hedley, M.J., and A. Metherell. 1995. Reactions controlling the cycling of P in soils. *In*: H. Tiessen (Ed.). Phosphorus in the global environment. Transfers, cycles and management. John Wiley and Sons Publishers, New York, NY. pp. 107-137.

Gerke, J, and R. Hermannn. 1992. Adsorption of orthophosphate to humic-Fe-complexes and to amorphous Fe-oxide. Z. Pflanzenernahr. Bodenk. 155:233-236.

Heckrath, G., P.C. Brookes, P.R. Poulton, and K.W.T. Goulding. 1995. Phosphorus leaching from soils containing different phosphorus concentrations in the Broadbalk experiment. J. Environ. Qual. 24:904-910.

Hesterberg, D., Hutchison, K., and S. Wang. 2004. Dissolution of ferrous iron and adsorbed phosphate during chemical reduction of iron oxide. Soil Sci. Soc. of N.C. 47th Annual Meeting. Raleigh, NC. (Oral Presentation).

Holford, I.C.R. and W.H. Patrick Jr. 1979. Effects of reduction and pH changes on phosphate sorption and mobility in an acid soil. Soil Sci. Soc. Am. J. 43:292-297.

Hughes, S. and B. Reynolds. 1991. Effects of clearfelling on microbial biomass phosphorus in the Oh horizon of an afforested podzol in Mid-Wales. Soil Use Mgmt. 7:183-188.

Husin, A.B., Caldwell, A.G., Mengel, D.B., and F.J. Peterson. 1987. Effects of natural and artificially induced reduction on soil solution phosphorus in rice soils. Plant & Soil. 102:171-175.

Kleinman, P.J.A., Needelman, B.A., Sharpley, A.N., and R.W. McDowell. 2003.Using Soil Phosphorus Profile Data to Assess Phosphorus Leaching Potential in Manured Soils. Soil Sci. Soc. Am. J. 67:215–224.

Koski-Vahala, J., and H. Hartikainen. 2001. Assessment of the risk of phosphorus loading due to resuspended sediment. J. Environ. Qual. 30:960-966.

Lindsay, W.L., Velk, P.L.G., and S.H. Chien. 1989. Phosphate minerals. pp. 1089-1130. *In*: Dixon, J.B. and S.B. Weed. (Eds.) Minerals in soil environment (2nd edition). SSSA Monograph. SSSA, Madison, WI.

Lindsay, W.L. 1979. Chemical equilibria in soils. John Wiley and Sons. New York, NY.

Mengel, K. 1985. Dynamics and availability of major nutrients in soils. Adv. Soil Sci. 2:65-131.

Mikkelsen, R.L. 1997. Agricultural and environmental issues in the management of swine waste. pp. 110-119. *In*: J.E. Rechcigl and H.C. MacKinnon (eds.) Agricultural uses of by-products and wastes. American Chemical Society. Washington, DC.

Moore, P.A. Jr., and K.R. Reddy. 1994. Role of Eh and pH on phosphorus geochemistry in sediments of Lake Okeechobee, Florida. J. Environ. Qual. 23:955-964.

NRCS. 1999. Natural Resources Conservation Service conservation practice standard: Nutrient Management. Code 590. Accessed September 12, 2004. http://www.ia.nrcs.usda.gov/technical/nutrientmanagementtools.html

Pant, H.K., and K.R. Reddy. 2001. Phosphorus sorption characteristics of estuarine sediments under different redox conditions. J. Environ. Qual. 30:1474-1480.

Pant, H.K., Reddy, K.R., and R.M. Spechler. 2002. Phosphorus retention in soils from a prospective constructed wetland site: environmental implications. Soil Sci. 167:607-615.

Patrick, W.H., Gotosh, S., and B.G. Williams. 1973. Strengite dissolution in flooded soils and sediments. Science. 179:564-565.

Patrick, W.H., Jr., and R.A. Khalid, 1974. Phosphate release and sorption by soils and sediments: Effects of aerobic and anaerobic conditions. Science 186:53-55.

Pena, F. and J. Torrent. 1990. Predicting phosphate sorption in soils of Mediterranean regions. Fertilizer Research. 23:17-19.

Phosphorus Loss Assessment Tool. NC State University. Accessed September 18, 2004. http://www.soil.ncsu.edu/nmp/ncnmwg/

Pierzynski, G.M., Logan, T.J., Traina, S.J., and J.M. Bigham. 1990. Phosphorus chemistry and mineralogy in excessively fertilized soils: Quantitative analysis of phosphorus-rich particles. Soil Sci. Soc. Am. J. 54:1576-1583.

Ponnamperuma, F.N. 1972. The chemistry of submerged soils. Adv. Agron. 24:29-96.

Rausch, C. and M. Bucher. 2002. Molecular mechanisms of phosphate transport in plants. Planta. 216:23-37.

Sallade, Y.E., and J.T. Sims. 1997. Phosphorus transformations in the sediments of Delaware's agricultural drainageways: II. Effect of reducing conditions on phosphorus release. J. Environ. Qual. 26:1579-1588.

Schwertmann, U. and Herbillon, A.J. 1992. Some aspects of fertility associated with the mineralogy of highly weathered tropical soils. *In*: Myths and science of soils of the tropics. SSSA Special Publication number 29. Madison, WI. Pp. 47-59.

Schwertmann, U., and R.M. Taylor. 1989. Iron Oxides. pp. 379-438, *In*: J.B. Dixon and S.B. Weed (eds.) Minerals in soil environment (2^{nd} edition). SSSA Monograph. SSSA, Madison, WI.

Sharpley, A.N., T.C. Daniel, and D.R. Edwards. 1993. Phosphorus movement in the landscape. J. Prod. Agric. 6, no. 4:492-500.

Sims, J.T., R.R. Simard, and B.C. Joern. 1998. Phosphorus loss in agricultural drainage: Historical perspectives and current research. J. Environ. Qual. 27:277-293.

Torrent, J., Schwertmann, U., and V. Barron. 1992. Fast and slow phosphate sorption by goethite rich natural materials. Clays Clay Miner., 40:14-21.

Vadas, P.A., and J.T. Sims. 1998. Redox status, poultry liter, and phosphorus solubility in Atlantic coastal plain soils. Soil Sci. Am. J. 62: 1025-1034.

Vadas, P.A., and J.T. Sims. 1999. Phosphorus sorption in manured Atlantic Coastal Plain soils under flooded and drained conditions. J. Environ. Qual. 28:1870-1877.

van der Zee, S.E.A.T.M., and W.H. van Riemsdijk. 1986. Sorption kinetics and transport of phosphate in sandy soil. Geoderma. 38:293-309.

van der Zee, S.E.A.T.M., and W.H. van Riemsdijk. 1988. Model for long term phosphate reaction kinetics in soil. J. Environ. Qual. 17:35-41.

White, R.E. 1982. Retention and release of phosphate by soil and soil constituents. *In*: Hucker, T.W.G., and G. Catroux (Eds.) Proceedings of a symposium on phosphorus in sewage sludge and animal waste slurries. D. Reidel Publishing Co., Dordrecht, The Netherlands. pp. 21-44.

Wild, A. 1950. The retention of phosphate by soils. A review. J. Soil Sci., 1:221-238.

Chapter Two: Reduction Reactor Experiments

INTRODUCTION

Particulate and dissolved phosphorus (P) loss from soils can result in P discharge into surface waters (Sharpley et al., 1993). Utilization of animal wastes as nutrient sources for agronomic crops has caused an excess of soil P in certain fields, since these wastes were historically applied based on the nitrogen contribution to the crop (Eghball and Power, 1999). Environmental concern over excessive levels of phosphorus in soils has caused the USDA-NRCS to regulate inputs of animal waste and fertilizers to agricultural fields. While environmental impacts and transport mechanisms of soil phosphorus have been studied (Correl, 1998, Sims et al., 1998), there are still many gaps in our knowledge about basic soil P chemistry. A more detailed understanding of these soil P process would lead to the development of more accurate best management practices (BMP's) for phosphorus in a variety of land-use scenarios. Scientifically sound BMP's and waste application policies are imperative to maintain the profitability of U.S. agriculture.

Research in the field of soil phosphorus chemistry has identified a process known as reductive dissolution of phosphate, or the dissolution of P from redox-active iron oxide minerals during reducing conditions (Patrick et al., 1973, Holford and Patrick, 1979, DeLaune et al., 1981, Husin et al., 1987, Sallade and Sims, 1997, Young and Ross, 2001). Due to the reduction potential of iron oxides, dissolution of these minerals is expected to increase greatly at soil redox potentials below 100 mV. For example, research has shown increased levels of dissolved iron during periods of sustained soil and iron oxide reduction (Gotoh and Patrick, 1974, Brennan and Lindsay, 1998, Gonzalez et al., 2002).

Sparks (1989) provides a series of sequential steps for reduction of metal oxides. These are (1) the diffusion of reductant molecules to the oxide surface, (2) surface chemical reaction, and (3) diffusion of reaction products from the oxide surface. This sequence can be expected during sufficiently reducing conditions.

Sallade and Sims (1997) conducted a laboratory incubation study in which sediments with varying degrees of P saturation were maintained under oxygen-free conditions for 21 days. A significant correlation was made between P and Fe in solution for certain soils in the study. Similar results were observed by Patrick (1973), DeLaune et al. (1981), Moore and Reddy (1994), and Vadas and Sims (1998).

Poorly crystalline iron oxides such as ferrihydrite have a high specific surface area, and a consequently high P sorption capacity (Patrick and Khalid, 1974, Borggaard, 1983, Pant and Reddy, 2001). Additionally, iron oxide crystallinity is negatively correlated with solubility (Gonzalez et al., 2002). The effects of P dissolution could therefore be more pronounced for phosphate associated with less crystalline iron oxide minerals under reducing conditions.

Because of their lack of redox activity, aluminum oxides are considered stable under reducing conditions (Darke and Walbridge, 2000). These minerals would also be expected to have P sorption characteristics that increase with decreasing Al-oxide crystallinity, since the more poorly crystalline aluminum materials possess greater surface areas (Richardson et al., 1988, Parfitt, 1989). For example, Darke and Walbridge (2000) found phosphate sorption to be highly correlated with oxalate-extractable aluminum in floodplain soils. Richardson (1985) found poorly crystalline Al-oxides to be the predominant sorbents of P in wetland environments, most likely due to the integrity

of these constituents during reduced conditions. Additional research has also highlighted the importance of Al-oxides as P sorbents at low redox potentials (Lockaby and Walbridge, 1998, Axt and Walbridge, 1999, Darke and Walbridge, 2000). Consequently, soils containing substantial amounts of poorly crystalline Al-oxide minerals could retain P regardless of redox conditions.

Since many studies indicate that iron and aluminum oxides are the most important constituents for P sorption in soils (reviewed by Beauchemin and Simard, 1999), and the aluminum oxide minerals should not be strongly influenced by reducing conditions, one could hypothesize that aluminum oxides may have a substantial effect on the net dissolution of P during reductive dissolution of Fe-oxides (and soils).

While a large body of literature supports the hypothesis of reductive P dissolution being associated with Fe-oxide reduction, other research has shown little correlation between reduced soil conditions and P in solution. Khalid et al. (1977) conducted a study in which soils were microbially reduced for 15 days. Dissolved phosphate did not increase during reduction. Vadas and Sims (1998) reported increases in dissolved P with reduction for portions of the soils in their study, but in other soils they reported decreases in dissolved P as Eh values decreased. Hutchison and Hesterberg (2004) found significant correlations between dissolved organic carbon (DOC) and phosphate, and speculated Fe-oxide dissolution as a less important mechanism for P dissolution than mechanisms involving DOC. Further research is needed to understand the processes and interactions involved in these reductive P dissolution processes.

Biotic reduction, or the utilization of soil organic matter (SOM) and external electron acceptors by native microbes in soils, is typically used in reductive P dissolution

experiments. Organic materials have been shown to enhance P sorption on mineral surfaces (Borggaard et al., 1990) and may form aqueous ternary complexes with Fe, Al and phosphate (Bloom, 1981, Gerke and Hermann, 1992). Other research has shown an inhibited sorption of P by Fe- and Al-oxides in the presence of organic materials due to competitive sorption between SOM and phosphate (Sibanda and Young, 1986, Violante et al., 1991). Consequently, SOM in soils may affect the dissolved P measured during reduction, and make the effect of the mineral reduction itself difficult to discern.

Studies investigating the effect of Fe- and Al-oxides exclusively on reductive P dissolution are lacking. Abiotic reduction using H_2 gas as a reducing agent has been reported in the literature (Collins and Buol, 1970, Amacher, 1991, Brennan and Lindsay, 1998). Reductive dissolution studies utilizing this type of reduction on pure mineral systems are appealing because complications arising from P interactions with soil organic matter can be avoided, and the precise role of iron and aluminum oxides in the reductive dissolution process can be investigated.

The goal of this research was to understand the role of Al-oxides on reductive P dissolution from Fe-oxides. Of particular interest was the specific interaction of P with ferrihydrite and boehmite during reduction. Ferrihydrite [$Fe(OH)_3$] and varying levels of boehmite (α-AlOOH) were reduced with dilute $H_{2(g)}$ for 72 h, and dissolved Fe(II) and phosphate were monitored. Subsequent experiments were conducted to determine potential mechanisms behind any effects of boehmite on P dissolution. The specific objectives were:

1. To determine the rate of reductive dissolution of ferrihydrite [synthetic ferric hydroxide - $Fe(OH)_3$] and dissolution of phosphate during

abiotic reduction of aqueous ferrihydrite/boehmite mixtures as affected by the concentration of boehmite (α-AlOOH).

2. To determine possible mechanisms affecting reductive P dissolution in ferrihydrite / boehmite mixtures.

MATERIALS AND METHODS

Mineral Synthesis and Characterization

Ferrihydrite [synthetic ferric hydroxide - $Fe(OH)_3$] and boehmite (α-AlOOH) were chosen for this work because of their high P sorption characteristics, and their similarity to poorly-crystalline secondary minerals responsible for most P retention in soils.

Ferrihydrite preparation

Ferrihydrite was synthesized following the procedure of Schwertmann and Cornell (1991). All solutions were made using analytical grade reagents and CO_2-free water prepared by boiling deionized water, then purging with $N_{2\ (g)}$ for approximately two hours. Two-hundred grams of $Fe(NO_3)_3 \cdot 9H_2O$ were dissolved in 2.5 L of deionized, CO_2-free water to produce a ferric iron solution. Five hundred milliliters of this solution were stirred and rapidly precipitated by adding 310 mL of 1 M KOH. This mixture was brought to pH 7.5 with standardized 0.01 M KOH using a calibrated pH electrode. This material was divided between six 250 mL polycarbonate centrifuge bottles, flushed with $N_{2\ (g)}$, and centrifuged for 15 minutes at 5,000 rpm. The above steps were repeated five times, until all 2.5 L of the $Fe(NO_3)_3 \cdot 9H_2O$ solution were utilized. After five batches of ferrihydrite were combined using centrifugation, 200 mL of 1 M KCl were added to each bottle and the sedimented pellet was dispersed using sonication. The samples were centrifuged once more at 5,000 rpm, and the supernatant solutions decanted. The ferrihydrite was washed twice with deionized water to lower the salt content, and inhibit the transformation to goethite (Cornell and Schneider, 1989). The pH of each sample was adjusted a final time to 7.0, and stored until combining into a final stock suspension.

Fifteen batches of ferrihydrite were synthesized as outlined above. The solids from each batch were then combined together into six, 250-mL centrifuge bottles. These samples were then washed twice with 0.01 M KCl and adjusted to pH 6.5. The stock suspension in each of these 250-mL bottles was then quantitatively washed into a 4 L storage container using 0.01 M KCl. The ferrihydrite was then brought to a total volume of 2 L using 0.01 M KCl, and the final pH was adjusted to 6.2. The ferrihydrite suspension was shaken on a reciprocating floor shaker to homogonize, flushed with N_2 gas in the bottle headspace before storage, wrapped in foil and stored at 4 ºC.

After the ferrihydrite stock was allowed to age for 2 weeks, the solids concentration was measured by heating subsamples of the well-mixed suspension for 24 h at 105 ºC and determining the mass of the subsamples before and after heating. This solids concentration determination was corrected for the amount of dried salt in the subsamples contributed by the 0.01 M KCl background.

Transformation During Storage

Transformation of ferrihydrite to a more crystalline material such as goethite was a concern for the stock mineral suspension. Previous research has shown that synthetic ferrihydrite may undergo these transformations, especially at higher temperatures (Schwertmann et al., 2000). To monitor crystallization changes in ferrihydrite over time, subsamples of the stock suspension were periodically analyzed for acid-soluble Fe (Cornell and Schneider, 1989).

An amount of stock suspension sufficient to give 0.1 g of solids was placed in a 250 mL polycarbonate centrifuge bottle. To each bottle, 100 mL of standardized 0.4 M

HCl was added (Cornell et. al., 1990, Tichang Sun et. al., 1996). The bottles were shaken at a temperature of 25 ºC for 30 minutes, and filtered through a 0.2-µm Millipore Isopore polycarbonate filter membrane (Millipore Corp., Bedford, MA). The iron present in solution was determined using a Perkin Elmer Model 3100 atomic absorption unit (Perkin Elmer Co., Boston, MA). The transformation of the ferrihydrite was expressed as Fe_A/Fe_T, where Fe_A is the acid dissolvable material, and Fe_T is the amount of iron calculated to be in the ferrihydrite sample based on the molecular weight of $Fe(OH)_3$.

As another means for monitoring the changes in the mineral suspensions over time, PO_4 sorption was measured periodically for one input level of P near the adsorption maximum for ferrihydrite and boehmite (2000 and 1200 mmol P kg^{-1} solids respectively). These samples were prepared in triplicate using the method described below.

Boehmite preparation

A boehmite stock suspension was prepared from pharmaceutical grade boehmite supplied as a suspension (Rehydragel HPA, Reheis Co., Berkeley Heights, NJ). One thousand grams of the commercial boehmite were added to a 2 L HDPE bottle. All aqueous solutions (1 M KCl, 0.01 M KCl, 0.01 M HCl, 0.01 M KOH) were prepared using CO_2 free deionized water as described above. To saturate the boehmite with K^+, an amount of KCl sufficient to yield a 1 M background (104.38 g) was added to the suspension, and the solution was shaken for 15 minutes at a rate of 1 s^{-1}. The pH of the suspension was adjusted to 6.0 using standardized 0.01 M HCl or KOH, and the material was shaken for 15 minutes more. The contents of this bottle were then divided evenly among six 250-mL polycarbonate centrifuge bottles and centrifuged for 15 minutes at

5000 rpm. The supernatant solution was discarded, and 120 mL of 1 M KCl were added to each bottle, and suspensions were adjusted to pH 6.0. The boehmite was washed three times with 0.01 M KCl, then shaken, centrifuged and compiled in a 2 L HDPE vessel. A solids concentration for the material was determined as outlined above. The boehmite stock suspension was shaken on a reciprocating floor shaker to mix, wrapped in foil and stored at 4 ºC. The headspace of the bottle was filled with N_2 gas before storage.

Phosphate adsorption isotherms

After the stock suspensions had aged for approximately one month, phosphate adsorption isotherms were performed using the basic procedure of Khare et al. (2004). Reagents for the experiment (0.01 M KCl, KH_2PO_4, HCl, and KOH) were prepared from CO_2-free deionized water. The experiment was conducted in 50-mL polycarbonate centrifuge tubes with a suspended solids concentration of 1.5 g kg^{-1}, an ionic strength of 0.01 mol L^{-1} KCl, and total sample mass of 30 g. Stock mineral suspensions were shaken for at least one half hour on a reciprocating floor shaker at a rate of 1 s^{-1} before being weighed into centrifuge tubes. Each sample was then brought to approximately 70% (20 g) of the final 30 g mass using 0.01 M KCl.

An appropriate amount of 0.01 M KH_2PO_4 was slowly added to each vigorously stirred sample in random chronological order to vary the amount of adsorbed PO_4. Samples were adjusted to pH 6.0 initially and periodically re-adjusted to pH 6.0 throughout a 40 h equilibration time. The samples were equilibrated on a reciprocating water bath shaker at a rate of 0.5 s^{-1} and a temperature of 22 ºC.

After 16 hours of shaking and pH adjustment, the samples were brought to a final mass of 30.0 g with 0.01 M KCl and equilibrated for 24 h more. Subsequent minor pH adjustments (< 0.2 pH units) involved trivial (microliter) additions of 0.01 HCl. The equilibrated samples were then centrifuged at 10,000 rpm for 15 minutes, and the supernatant solutions were decanted. The pH of an aliquot of each supernatant solution was measured. The supernatant solutions were then filtered through 0.2-µm Millipore Isopore polycarbonate vacuum filter membranes, and analyzed for PO_4 using the molybdate colorimetric procedure (Olsen and Sommers, 1982). The amount of phosphate sorbed to the mineral was computed as the difference between the total added PO_4 and the PO_4 measured in the equilibrium solution.

Redox Reactor Experimental Design

Reduction reactor experiments were conducted in a continuously stirred, pH-controlled reactor system as illustrated in Figure 2.1. Mineral suspensions were contained in a 2-L, water-jacketed glass reactor vessel (Wilmad-Labglass Corp., Buena, NJ). A constant temperature of 20 ºC was maintained by a circulating water bath system. The pH of the reactor suspension was maintained at 6.0 by a Radiometer Analytical Model TM 850 Autotitrator (Radiometer Analytical Corp., Lyon, France) with reservoirs of 0.01 M HCl or KOH. Through the four-holed lid of the reactor vessel was inserted a pH and Eh electrode, each through a single rubber stopper. Another stopper with multiple entries housed a thermometer, vent port, sampling tube, and gas dispersion tube. Acid and base dispensing tips from the pH controller were inserted directly into the top of

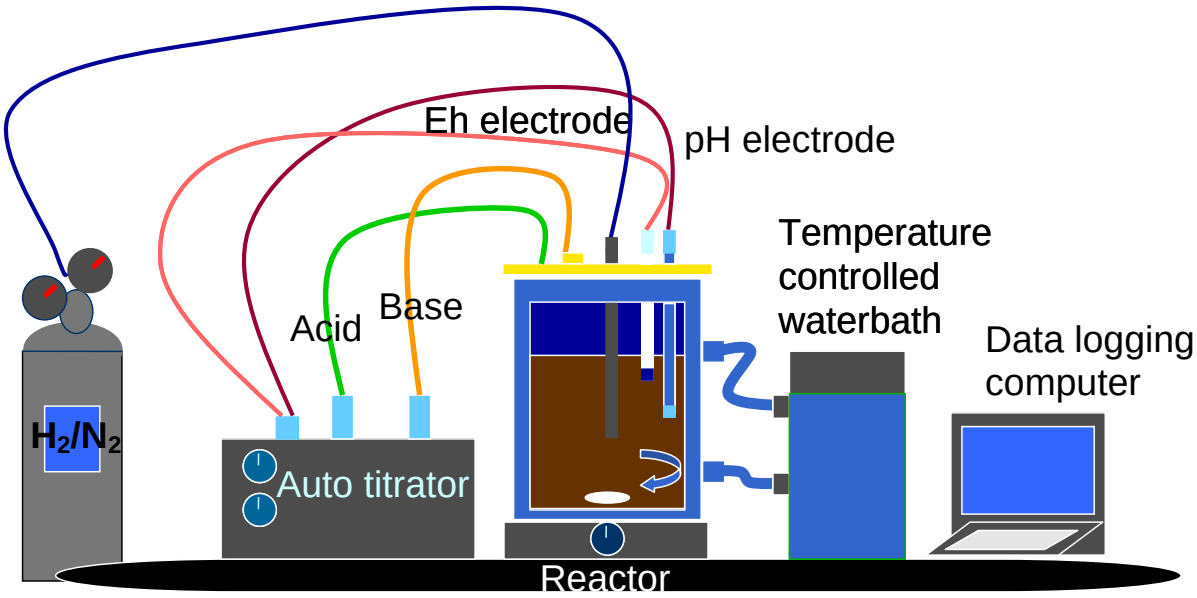

Figure 2.1. Schematic of reactor system used to complete single and mixed mineral reductive dissolution experiments.

the reactor vessel (Figure 2.1). Reagents for the experiment (0.01 M KCl, KH_2PO_4, HCl, and KOH) were prepared from CO_2-free deionized water. The mineral suspension in the reactor was equilibrated with phosphate under $N_{2\,(g)}$ for 24 hours, then reduced for 72 hours.

Abiotic reduction was accomplished using dilute H_2 in $N_{2(g)}$ (0.5%), as used by others (Collins and Buol, 1970, Brennan and Lindsay, 1998). Following Brennan and Lindsay (1998), 10% platinum on activated carbon catalyst (Sigma Aldrich Co., Milwaukee, WI) was added to each reactor system at a rate of 0.25 g g^{-1} ferrihydrite to enhance electron transfer to the iron oxide mineral.

Mixtures of ferrihydrite and boehmite were used in the reduction experiments. One liter suspensions contained 0.5 g ferrihydrite clay and between 0 and 0.7 g boehmite (Table 2.1). The concentration of ferrihydrite was kept constant so that an equal amount of reducible mineral would be present in each system. Each stock mineral suspension was shaken for at least 30 minutes before weighing into a tared, 2-L HDPE bottle. As in isotherm experiments, the sample was brought to approximately 70% of the final mass with 0.01 M KCl and stirred rapidly on a magnetic stirrer. An appropriate amount of KH_2PO_4 solution was added to this suspension to yield 750 mmol P per g of ferrihydrite clay in the system (Table 2.1). The suspension was then manually brought to pH 6.0 with 0.01 M HCl or KOH, and brought to a final mass of 1 kg with 0.01 M KCl. Suspensions were then transferred from the HDPE bottle to the 2-L, glass reactor vessel.

The autotitrator device was set to maintain a constant pH of 6.0 throughout the duration of a given experiment using electrodes that were cleaned with pH 3.0

ammonium oxalate and re-calibrated daily. Eh was monitored with platinum electrodes that were also cleaned and checked daily.

Table 2.1. Experimental parameters for 72 h reactor systems. All systems contain 0.5 g ferrihydrite and 750 mmol PO_4 added per kg of ferrihydrite in the system.

Mass of boehmite solids (g)	**P sorption capacity from both minerals* (µmol)**	**Sorption capacity from boehmite* (%)**
0	800	0
0.002	801.3	0.2
0.004	802.6	0.3
0.008	805.2	0.6
0.02	813	1.6
0.08	852	7
0.2	930	16
0.3	995	20
0.7	1255	36

*Total sorption capacity in reactor based on P sorption capacities of 1600 and 650 mmol P kg^{-1} ferrihydrite and boehmite respectively at the beginning of the experimental period.

Reactor suspensions were equilibrated for 24 h under 99.99% pure N_2 gas flowing at a rate of 100 mL min^{-1}. After this 24 h equilibration, platinum on activated carbon catalyst was added at a rate of 0.25 g g^{-1} of ferrihydrite clay. After equilibrating with the Pt catalyst for an additional hour, a sample was collected representing time zero of the 72-hour reduction period. The gas flow was then switched to 0.5% H_2 in $N_{2(g)}$ flowed at a rate of 100 mL min^{-1} for the duration of the experiment. Samples were collected from 0 h up to 72 h as described below.

Sampling and Analysis

Periodic reactor samples were collected through a sampling tube inserted into the reactor suspension through one of the access holes in the glass redox reactor top. A glass syringe was used to remove 25 mL of the reactor suspension. This suspension was filtered under vacuum through a 0.2-µm Millipore Isopore polycarbonate filter membrane in a N_2 purged glovebox (Figure 2.2). This process was done under a safelight to inhibit photo-oxidation of any reduced iron in the suspension or filtrate. The filtrate was transferred into a 50 mL evacuated amber-colored serum bottle. Portions of the filtrate were analyzed for dissolved ferrous iron and phosphate as described below.

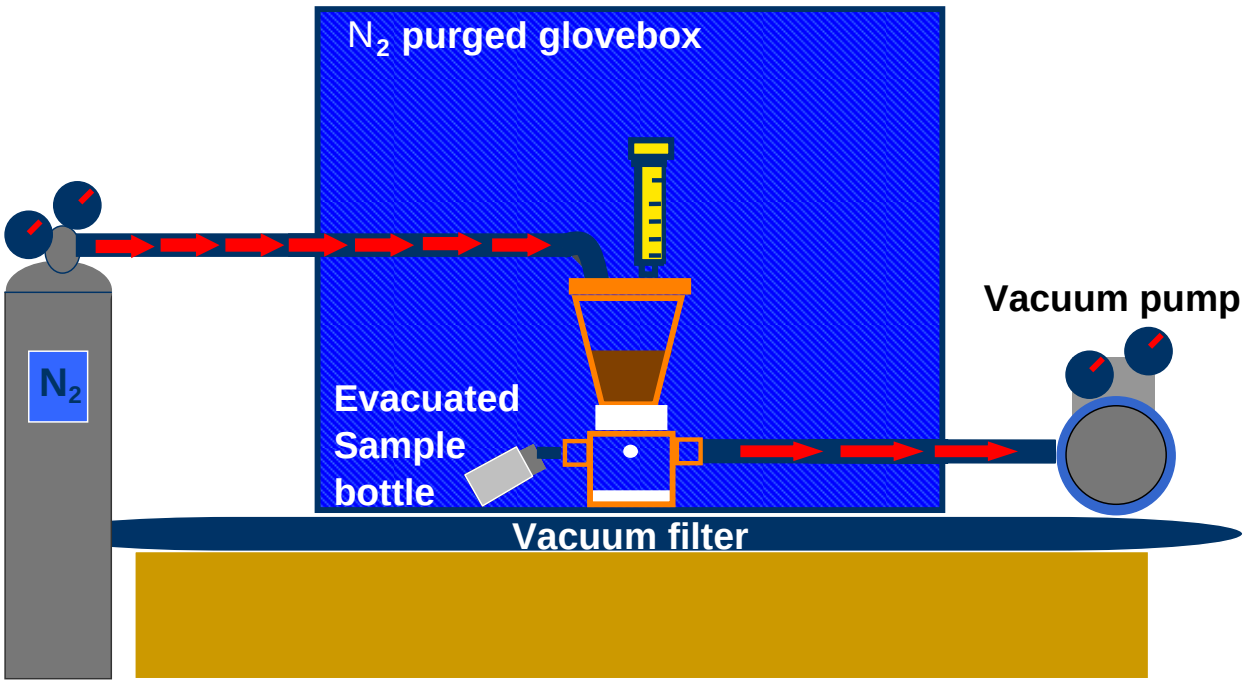

Figure 2.2. Schematic of glovebox sampling apparatus used to prevent oxidation during ferrous iron complexation by phenanthroline.

Ferrous iron analysis

The phenanthroline colorimetric method was employed for ferrous iron analysis as described by Olsen and Ellis (1982). Phenanthroline complexation of Fe(II) was conducted in an N_2 purged glove box under a safelight. Standards were generated by mixing combinations of a ferrous iron solution, concentrated HCl, 1,10 phenanthroline, ammonium acetate buffer, and 1 M KCl solutions in 50 mL volumetric flasks. Samples were prepared with the same reagents, excluding the ferrous iron solution.

Ferrous iron solution was prepared by dissolving 0.1755 g of ferrous ammonium sulfate in deionized water and bringing to 250 mL in a volumetric flask. Phenanthroline was prepared by simultaneously heating and stirring 0.100 g of 1, 10 phenanthroline reagent in 75 mL of deionized water in a 100 mL volumetric flask. After the material had dissolved, the flask was allowed to cool, and brought to volume with deionized water. The ammonium acetate buffer was prepared by dissolving 250 g of ammonium acetate into 150 mL of deionized water and adding 700 mL of glacial acetic acid.

Absorption of samples and standards were analyzed at a wavelength of 510 nm on a Shimadzu Model UV 2101-PC Spectrophotometer (Shimadzu Corp., Colombia, MD) using a 1-cm path cell.

Phosphate analysis

Phosphate was analyzed using the molybdate colorimetric (Murphy-Riley) procedure (Murphy and Riley, 1962, Olsen and Sommers, 1982). Two standard reagents were used for standard curves and samples. Reagent A was prepared by combining 1 L of 5 N H_2SO_4 with 12 g of ammonium paramolybdate dissolved in 250 mL of deionized

water and 0.29 g of potassium antimony tartarate into 100 mL of deionized water. This solution was brought to a total volume of 2 L and stored in a walk in cooler at 4°C to prevent chemical transformations. Reagent A was combined with 0.528 g of ascorbic acid to generate reagent B. Standards in concentrations of 0 to 1.0 mg L^{-1} were prepared from concentrated secondary standards composed of primary 1,000 mg L^{-1} P standard (Fisher Scientific, Fairlawn, NJ), 10 mM KCl and the coloring reagent B. Samples were prepared by weighing a portion of the sample filtrate into a 50 mL volumetric flask. Eight mL of the coloring reagent B was added, and samples were brought to the final 50 mL volume with 10 mM KCl. The samples were analyzed at a wavelength of 840 nm on a Shimadzu Model UV 2101-PC Spectrophotometer (Shimadzu Corp., Colombia, MD) using a 1 or 5-cm path cell.

Supporting Experiments

Additional experiments were conducted to elucidate mechanisms behind the observed inhibition of Fe(II) and P dissolution in the presence of boehmite. The details of these experiments are described below.

Ferrous Iron Sorption on Boehmite

To evaluate the ability of boehmite to scavenge dissolved ferrous iron, an adsorption isotherm experiment was conducted. Reagents for the experiment (0.01 M KCl, $FeCl_2 \cdot 4H_2O$, HCl, and KOH) were prepared from CO_2-free deionized water. Ferric chloride solution was prepared the day of the experiment to limit oxidation. The experiment was conducted in 250-mL polycarbonate centrifuge bottles with a suspended

solids concentration of 0.5 g kg^{-1}, an ionic strength of 0.01 mol L^{-1} KCl, and total sample mass of 30 g. The stock boehmite suspension was shaken for at least half an hour on a reciprocating floor shaker at a rate of 1 s^{-1} before being weighed into centrifuge tubes. These samples were then brought to approximately 70% of the final mass using 0.01 M KCl.

An appropriate amount of 0.01 M $FeCl_2 \cdot 4H_2O$ was added to each vigorously-stirred sample in random chronological order to vary the amount of adsorbed ferrous iron. Samples were adjusted to pH 6.0 initially, and periodically re-adjusted to pH 6.0 throughout a 24 h equilibration time. Sample equilibration was done on a reciprocating water bath shaker at a rate of 0.5 s^{-1} and a temperature of 22 ºC. Additions of $FeCl_2 \cdot 4H_2O$, and any subsequent pH adjustments were conducted in an N_2 purged glovebox.

After 4 hours of shaking and pH adjustment, the samples were brought to a final mass of 30.0 g with 0.01 M KCl and equilibrated 20 h more. The equilibrated samples were then centrifuged at 5,000 rpm for 15 minutes, and the supernatant solutions were decanted in an N_2 purged glovebox. The pH of the supernatant solutions was quantified using a small aliquot of the supernatant. The supernatant solutions were then filtered through 0.2-µm Millipore Isopore polycarbonate vacuum filter membranes following the protocol for redox reactor samples, and analyzed for Fe(II) using the phenanthroline colorimetric method (Olsen and Ellis, 1982). The amount of ferrous iron sorbed to the mineral was computed as the difference between the total added Fe(II) and the Fe(II) measured in the equilibrium solution.

Solid Phase P Speciation

To detect transfer of P between ferrihydrite and boehmite during reduction of mineral mixtures, X-ray absorption near edge structure (XANES) spectroscopy was utilized. A reactor system analogous to that described above containing 0.9 g each of ferrihydrite and boehmite was reduced for 168 h under 0.5 % H_2 in N_2 gas. A 1:1 mineral mixture was chosen for this system to detect transfers of P between the two minerals during reduction. Phosphate was added to the system as 0.01 M KH_2PO_4 at a rate of 750 mmol P per kg of total solids in the system, and equilibrated for 24 h prior to the start of reduction. At 0, 24, 72, 92, 144 and 168 h, 25 mL samples were collected and analyzed for ferrous iron and phosphate as described above. A 100 mL sample was also withdrawn and centrifuged in a 250 mL polycarbonate bottle at a rate of 5,000 rpm for 15 minutes. These centrifuged solids were transferred with a portion of supernatant to a 50 mL polycarbonate centrifuge tube and centrifuged for an additional 15 minutes at a rate of 15,000 rpm. While working in an N_2-purged glovebox, a portion of the clay was thoroughly mixed and dewatered to a paste consistency on a 0.2-µm vacuum filter, placed into acrylate sample holders for XANES analysis, and covered with 5-µm thick polypropylene X-ray film (Spex Industries, Metuchen, NJ).

In addition to the periodic samples, mineral standards with sorbed P at 500 mmol kg^{-1} boehmite and 1000 mmol kg^{-1} ferrihydrite were prepared following the protocol for 42 h phosphate adsorption isotherms detailed above. At the end of the 42-hour equilibration, the clay from the centrifuged samples was placed into an acrylate sample holder.

Data Collection

Samples were analyzed at Beamline X19A at the National Synchrotron Light Source (NSLS), Brookhaven National Laboratory, Upton NY. An electron beam energy of 2.5 GeV and a maximum beam current of 300 mA were utilized for analysis. A Si (111) monochromater was used to monochromatize the radiation generated from the synchrotron ring, and detuned 50%. This monochromater was calibrated to 2149 eV at the phosphors K edge using a variscite reference standard (400 mmol P kg^{-1}), and the calibration was re-checked with this standard after analyzing every fourth sample. Data were collected from 2119 to 2249 eV using a step size of 0.2 eV between 2119 and 2139 eV, 0.05 eV from 2139 to 2154 eV, 0.1 eV from 2155 to 2179 eV and 1.0 eV from 2180 to 2249 eV. Two to four scans with consistent baselines were averaged. The scans were collected in fluorescence mode using a Passivated Implanted Planar Silicon (PIPS) detector mounted into a $He_{(g)}$ purged chamber to prevent X-ray attenuation.

Data Analysis

The raw data were baseline corrected using the Athena XANES analysis software (Newville, 1997). All spectra were single point background normalized at the energy of the maximum peak between 10 and 18 eV in the first derivative XANES spectrum following the procedure of Khare et al. (2004). The spectra were then adjusted to a common florescence yield value at –8 eV.

Least squares linear combination fitting was conducted using the software package Kaleidagraph (Synergy Software, Reading, PA). Hesterberg et al. (1999) showed characteristic features in the spectra of iron phosphate species at -3 eV (relative

energy), just before the intense white line peak of 2150 eV for phosphorus. Distinct features that are present in this region for Fe-phosphate minerals are absent in Al-phosphate minerals. Khare et al. (2004) used this information to determine the preference of phosphate for Fe- and Al-oxides in mixed mineral systems. These pre-edge features were therefore used to determine the distribution of P in this experiment. The spectra collected over the course of the 168 h reduction experiment were fit with spectra for standards of 500 mmol kg^{-1} P on boehmite and 1000 mmol kg^{-1} on ferrihydrite.

Dissolved Aluminum Reactor Systems

To test the hypothesis of ferrihydrite reduction inhibition by dissolved Al(III) from boehmite, reactor experiments were conducted with $AlCl_3$ inputs analogous to the moles of Al(III) in 0, 0.002, 0.008 and 0.08 g boehmite (assuming complete dissolution).

Each ferrihydrite stock suspension was shaken for at least 30 minutes before 0.5 g were weighed into a tared, 2-L HDPE bottle. The sample was brought to approximately 50 % of the final mass of 1 kg with 0.01 M KCl and stirred rapidly on a magnetic stirrer. The suspension pH was then taken to 3.0 with 0.01 M HCl to prevent precipitation of Al-hydroxide upon adding the $AlCl_3$ solution. Aluminum chloride (0.01 mM) solution was added to this suspension to yield the desired input Al concentration of 0, 67, 267 or 2,667 mmol kg^{-1} ferrihydrite which was equivalent to the Al added in the 0, 0.002, 0.008 and 0.08 g mixed mineral systems assuming complete boehmite dissolution. The suspension was then brought to 70 % of the final mass with 0.01 M KCl, and a 25 mL subsample was withdrawn with a glass syringe to quantify the amount of Al(III) sorbed to the

ferrihydrite as that portion of Al(III) lost from solution. The suspension was then manually brought to pH 6.0 and a final mass of 1 kg with 0.01 M KOH and 0.01 M KCl respectively, and transferred from the HDPE bottle to the 2-L, glass reactor vessel.

Reactor suspensions were equilibrated for 24 h under N_2 gas flowing at a rate of 100 mL min^{-1}. After this 24 h equilibration, 10 % platinum on activated carbon catalyst was added at a rate of 0.25 g g^{-1} of ferrihydrite clay. After equilibrating with the Pt catalyst for an additional hour, 0.5 % H_2 balanced with N_2 gas was flowed through the system at a rate of 100 mL min^{-1} to induce reduction, and a sample was collected representing time zero of the experiment. Sampling and analysis occurred as described for the mixed mineral reduction reactor experiments from 0 to 48 hours.

Platinum Catalyst Sorption of Al(III)

To evaluate the effect of sorbed Al(III) on the catalytic activity of the 10 % Pt on activated carbon catalyst, a 24-h sorption experiment with Al(III) was conducted. A mass of catalyst sufficient to yield a final suspended solids concentration of 1.25 g kg^{-1} suspension (0.1625 g) was added to two 250 mL polycarbonate centrifuge bottles. The bottles were then brought to approximately 30 % of the final volume of 130 mL with 0.01 M KCl and shaken for 30 minutes to hydrate. The pH of the suspensions was then brought to pH 3.6 with 0.01 M HCl to prevent precipitation of Al-hydroxide upon adding $AlCl_3$ to the catalyst. Zero and 3.3 mL of 10 mM $AlCl_3$ was then added to each sample. The latter input was the equivalent amount of Al(III) that could be sorbed to the catalyst surface (266 mmol kg^{-1}) in the mixed-mineral system containing 0.008 g boehmite if this

mineral completely dissolved. The pH of each sample was measured after $AlCl_3$ addition, and the 0 mL input system was brought to the same pH as the 3.3 mL system.

The catalyst suspensions were then brought to 70 % of the final mass with 0.01 M KCl, and equilibrated on a reciprocating water bath shaker at 25 ºC for 4 hours. The pH was again adjusted to pH 3.6 after this 4-h equilibration, and the catalyst suspensions were then brought to a final mass of 130 g before being equilibrated for an additional 20 hours.

After the 24 hour equilibration, 30 mL of each catalyst suspension was removed, centrifuged and filtered to determine catalyst sorption of Al(III) as that portion of Al lost from solution. The remaining 100 mL of catalyst suspensions were added to each of two pre-equilibrated redox reactor systems containing 700 mL of ferrihydrite suspension (0.4 g ferrihydrite), through which N_2 gas was flowed. A final pH of 6.0 and mass of 1 kg for each reactor suspension was achieved by adding 0.01 M KOH and KCl respectively. The ferrihydrite suspensions were then reduced with 0.5 % H_2 balanced with N_2 gas and sampled from 0 to 48 hours as outlined above.

Statistical Analysis

Linear regression models were computed using KaleidaGraph software. Other statistical computations were conducted with SAS software, version 8.2 (SAS Institute, 1999) using PROC CORR, PROC REG, or PROC GLM.

RESULTS

Stock Suspension Isotherms and Monitoring

Phosphate adsorption isotherms conducted on the stock mineral suspensions 15 days after stock preparation appear in Figure 2.3. Isotherms were L curves, and a Freundlich isotherm model was fit to adsorption data for both minerals. The maximum PO_4 adsorption capacity of ferrihydrite (1900 mmol kg^{-1}) was almost three times more than that of boehmite (650 mmol kg^{-1}).

The results of acid extractable Fe from ferrihydrite and maximum P sorption capacity measurements for ferrihydrite and boehmite appear in Table 2.2. Linear regression analysis was performed on the temporal trends of these stock suspension measurements, and are shown in Figures A.1 and A.2. A significant linear ($R^2 = 0.93$; $p = 0.05$) decrease in the proportion of acid extractable Fe from ferrihydrite was noted from 0.44 (4.1 mmol kg^{-1}) at 120 days, to 0.31 (2.9 mmol kg^{-1}) at 620 days (Figure A.1). Significant linear ($R^2=0.76$; $p < 0.01$) decreases over time were also observed in the maximum phosphate adsorption capacity of ferrihydrite (1900 to 1200 mmol kg^{-1} at 10 and 280 days respectively, Table 2.2; Figure A.1). No significant change in maximum P adsorption capacity for boehmite in the stock suspension was observed during the monitoring period (Figure A.2).

Because of the effects of crystallinity on P sorption capacity of the ferrihydrite, a correlation between decreased acid dissolvable Fe (indicative of enhanced crystallinity) and decreased P sorption capacity might be expected for the ferrihydrite stock suspension.

No statistically significant correlation was observed however, likely due to a lack of statistical power for this comparison (n = 4, 2 df; Figure A.3).

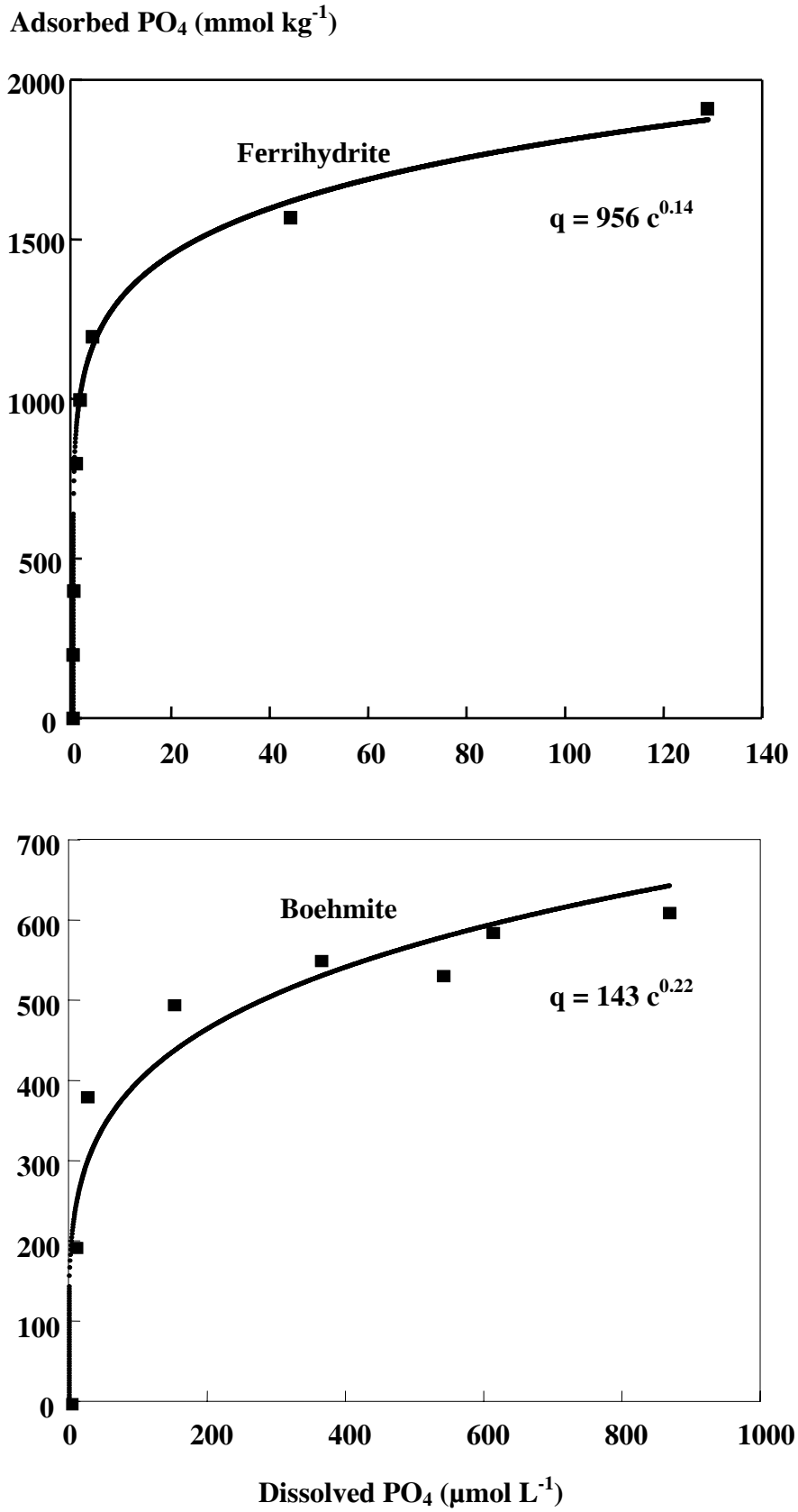

Figure 2.3. Adsorption of PO_4 on ferrihydrite or boehmite at pH 6.0 in 0.01 M KCl background after 40 h of equilibration. Smooth curves are Freundlich model fits to the data.

Table 2.2. Temporal changes in selected properties of ferrihydrite and boehmite suspensions stored at pH 6 in 0.01 M KCl background

Stock Suspension[a]	**Time in Stock Suspension (d)**	**Crystallinity**[b] **(Fe_A/Fe_T)**	**P adsorbed**[c] **(mmol kg^{-1})**
Ferrihydrite	10	no data	1911 ± 18
	120	0.44 ± 0.07	1743 ± 15
	180	0.37 ± 0.03	1877 ± 45
	500	0.35 ± 0.01	1392 ± 28
	530	no data	1324 ± 13
	560	0.35 ± 0.09	1211 ± 33
	620	0.31 ± 0.03	no data
Boehmite	10	n/a	609 ± 6
	40		633 ± 7
	70		586 ± 9
	100		610 ± 0.4
	160		599 ± 9
	220		660 ± 13
	250		629 ± 0.7
	280		583 ± 11

[a] Ferrihydrite suspension was prepared September 2002, Boehmite suspension prepared June 2003.

[b] Fe_A- Portion of Fe in ferrihydrite extractable with 0.4 M HCl; Fe_T - Theoretical total Fe (9.3 mmol kg^{-1}) based on chemical formula of $Fe(OH)_3$ for the synthesized ferrihydrite (Cornell and Schneider, 1998).

[c] P input of 2000 and 1200 mmol kg^{-1} for ferrihydrite and boehmite respectively

Reduction Reactor Experiments

General Trends

Figure 2.4 shows trends in Eh, and dissolved iron and phosphate for a redox reactor system containing ferrihydrite only (0 g boehmite). Typical of all the reduction experiments, Eh decreased to approximately –200 mV. Dissolved phosphate showed a significant increase with time ($R^2 = 0.92$; $p < 0.01$) with decreasing Eh. The maximum dissolved PO_4 at the end of 68 h of reduction was 15 µmol L^{-1} (0.46 mg L^{-1}). Dissolved ferrous iron also showed a significant linear increase with time ($R^2 = 0.94$; $p < 0.01$) during reduction, and a maximum of 1,800 µmol L^{-1} of dissolved Fe(II) was measured at 68 h.

Figure 2.5 shows trends in Eh, and dissolved phosphate and aluminum for a control system with 0.5 g boehmite and no ferrihydrite. Dissolved aluminum was not detected (< 4.4 mg L^{-1}) in this system. Dissolved phosphate decreased over time ($R^2 = 0.94$; $p < 0.01$) during reduction.

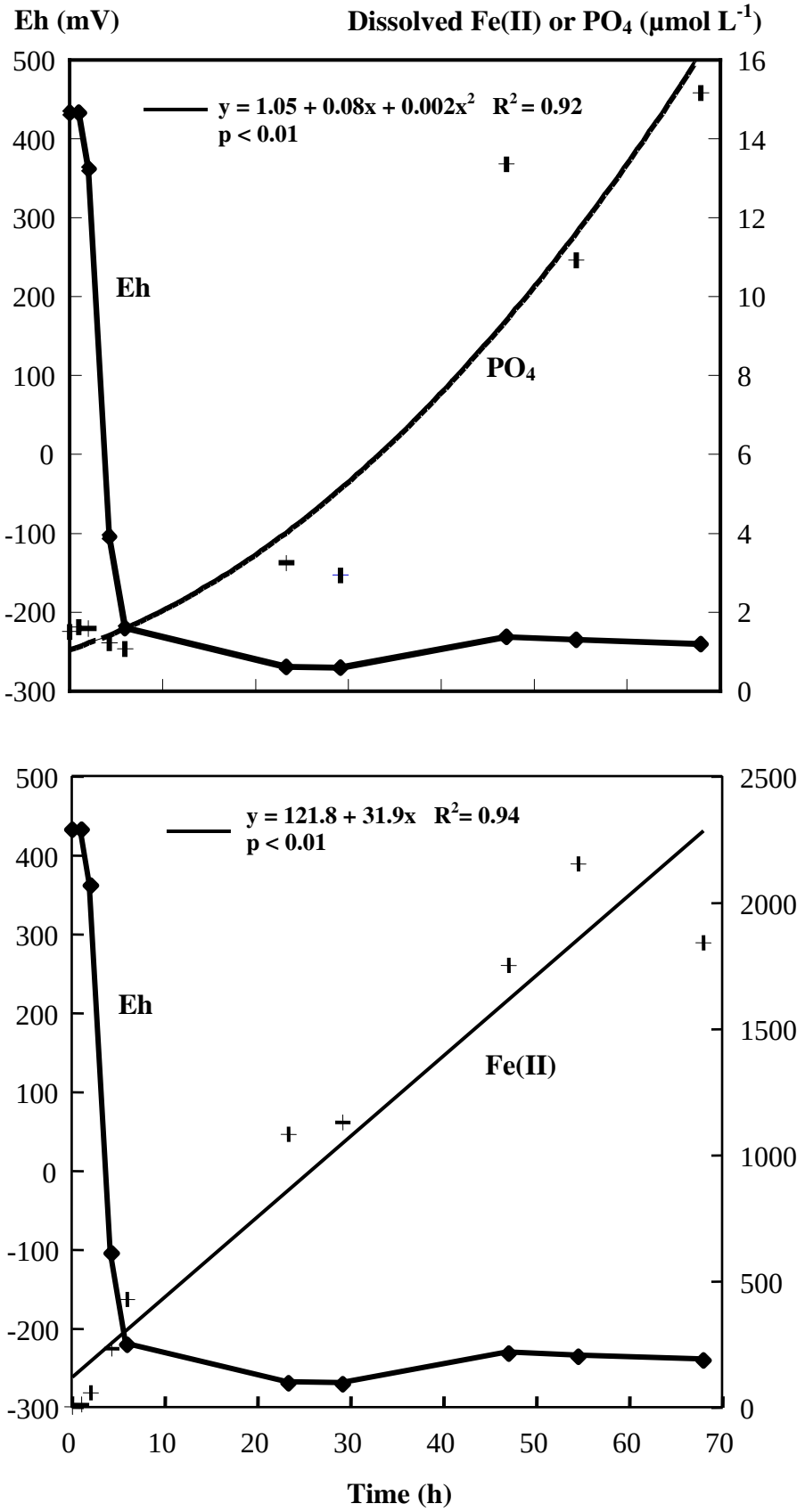

Figure 2.4. Trends in Eh, and dissolved Fe(II) and P for a 68-h reduction experiment with 0.5 g ferrihydrite, 0 g boehmite and 750 mmol P kg^{-1} solids.

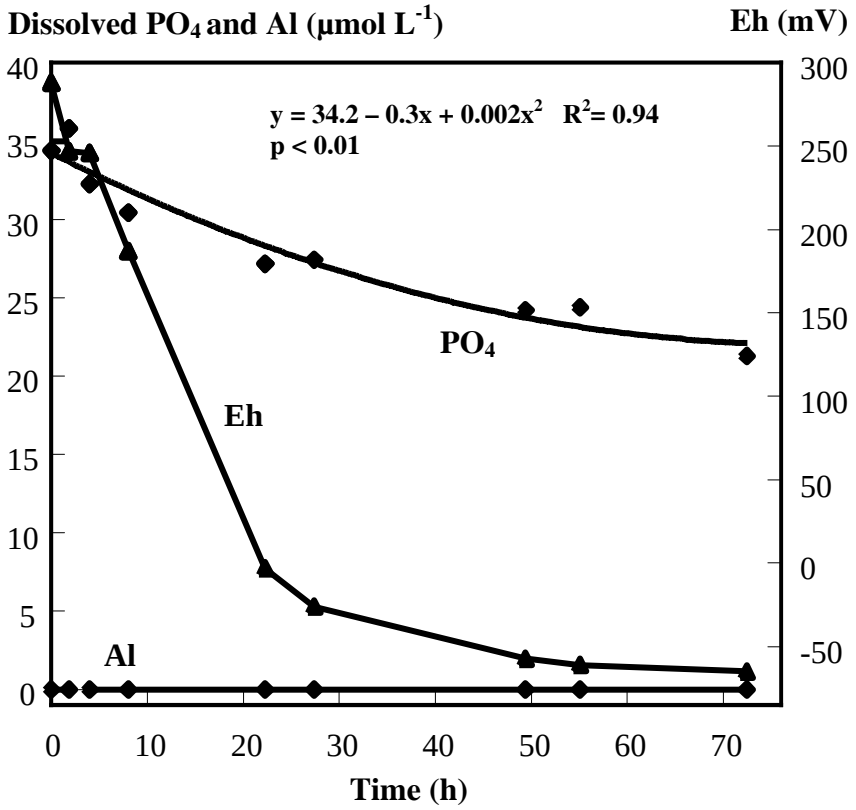

Figure 2.5. Trends in dissolved P and Al during a 72-h reduction experiment with 500 mmol P kg^{-1} solids, 0.5 g boehmite, and 0 g ferrihydrite.

Dissolved Ferrous Iron

Trends in dissolved ferrous iron for mixed ferrihydrite/boehmite mineral systems containing between 0 and 0.008 g boehmite are shown in Figure 2.6. Significant correlations between dissolved ferrous iron and time were seen in each of these systems ($R^2 > 0.90$; $p < 0.01$). A decrease in Fe(II) dissolution was observed between 0 and 0.008 g boehmite. Additionally, significant ($p = 0.05$) differences in the slopes of the zero order linear models were observed between the 0 and 0.002 g and 0.002 and 0.008 g systems, indicating that boehmite inputs as low as 250-fold less than that of ferrihydrite had an effect on ferrous iron dissolution in these mixed-mineral systems.

The decrease in ferrous iron dissolution with increasing boehmite was less pronounced from 0.02 to 0.7 g boehmite (Figure A.4). Significant correlations between dissolved ferrous iron and time were not observed in these systems. A significant ($p = 0.05$) difference in the rate of Fe(II) dissolution (taken as the difference in slopes of the zero order linear models) was observed between the 0.008 and 0.02 g systems, while no significant differences among dissolution rates were seen between any of the systems from 0.02 to 0.7 g.

The rate coefficients determined from zero order kinetic models fit to the dissolved Fe(II) data from each experiment appear in Table 2.3. Trends in these rate coefficients for dissolved ferrous iron are shown in Figure 2.7. A linear decrease in Fe(II) dissolution rate was observed from 0 to 0.008 g boehmite ($R^2 = 0.61$). This decrease was not statistically significant however, probably due to a small number of data points ($n = 4$) and a subsequent lack of statistical power ($df = 2$) for this linear model. Systems containing 0.02 to 0.7 g of boehmite showed negligible Fe(II) dissolution (rate

coefficients approximately zero, Table 2.3), and were not correlated with boehmite concentration ($R^2 = 0.34$, $p > 0.05$; Figure 2.7).

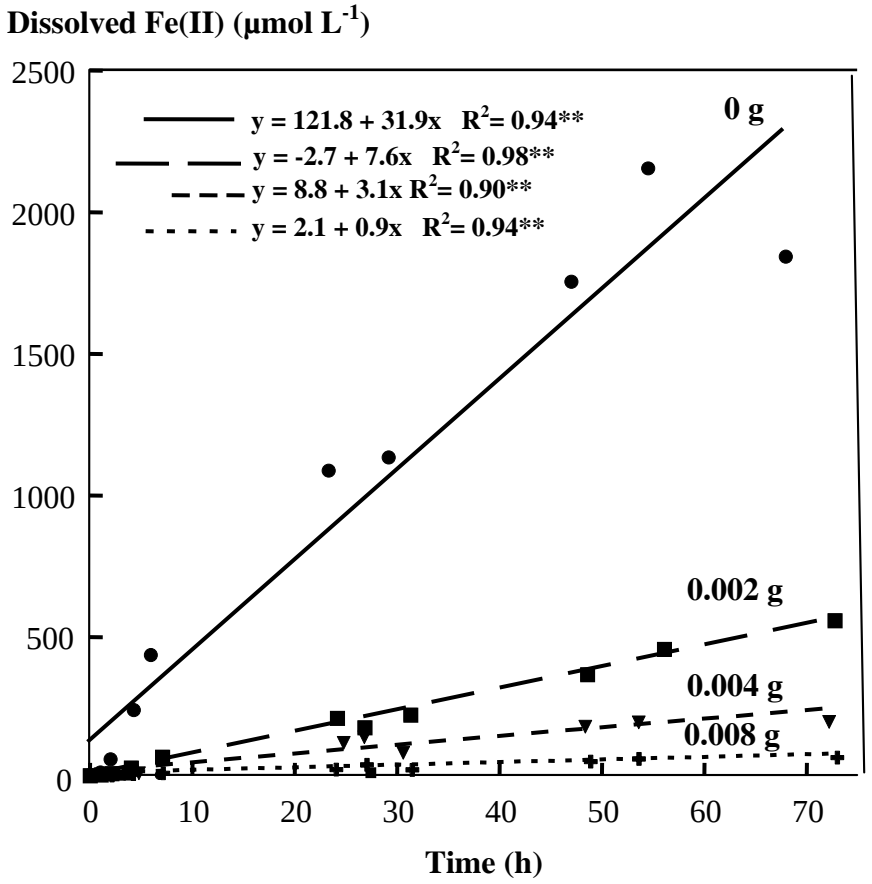

Figure 2.6. Trends in dissolved Fe(II) over time for 72-h redox reactor experiments with 0.5 g ferrihydrite, 0 to 0.008 g boehmite, and 750 mmol P kg^{-1} solids. **$p < 0.01$

Table 2.3. Rate coefficients of kinetic models fit to dissolved Fe(II) and P data in systems with 750 mmol P kg^{-1} solids, 0.5 g ferrihydrite, and 0 to 0.7 g boehmite.

Mass of boehmite (g)	Fe(II) Rate Coefficient[a] (µmol L^{-1} h^{-1})	P Rate Coefficient[b] (µmol L^{-1} h^{-1})
0	38.1	0.04
0.002	7.6	-0.01
0.004	3.1	-0.02
0.008	0.93	-0.03
0.02	0.12	-0.03
0.08	0.016	-0.01
0.2	-0.032	-0.02
0.3	0.005	-0.05
0.7	-0.017	-0.001

[a]Zero order kinetic model
[b]First order kinetic model

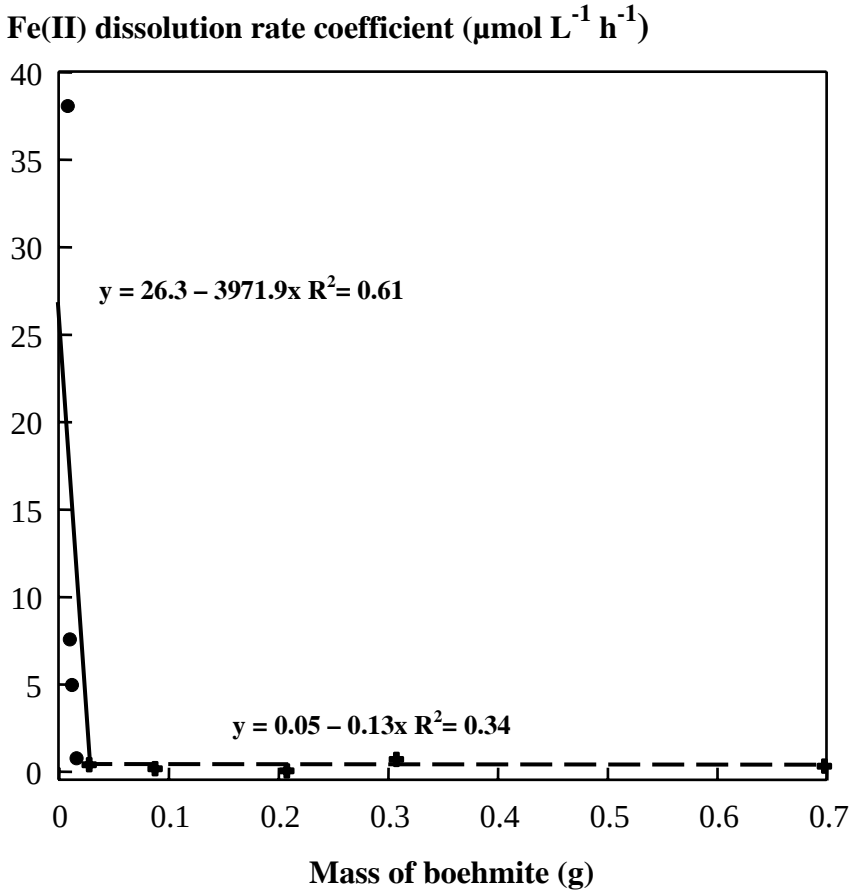

Figure 2.7. Trends in rate coefficients of zero order kinetic models fit through dissolved Fe(II) data for mixed mineral systems with 0.5 g ferrihydrite, 0.002 to 0.7 g boehmite, and 750 mmol P kg^{-1} solids.

Dissolved Phosphate

Figure 2.8 shows the trends in selected ferrihydrite-boehmite systems with 750 mmol P kg^{-1} solids. The system containing 0 g boehmite showed a net increase in dissolved P over time, with a maximum of 15 µmol P L^{-1} at the cessation of reduction. Unlike the 0 g boehmite system, no increase in dissolved phosphate over time was observed in systems containing boehmite (Figures 2.5 and 2.8). These systems exhibited the maximum dissolved phosphate at the beginning of reduction, and showed a decrease in the amount of dissolved P over time, suggesting that uptake of P occurred.

Because of the apparent lack of linearity in dissolved P at the beginning of reduction, first order kinetic models were fit to the P data for mixed mineral systems (Table 2.3). These models were significant ($p < 0.01$) with the exception of the 0.2 and 0.7 g systems (Figure A.5). Negative values from these kinetic models were indicative of net P uptake in these systems. The trends of these P uptake rate coefficients as a function of added boehmite are displayed in Figure 2.9. No significant ($p = 0.05$) relationship was found between P uptake rate and added boehmite concentration.

Correlations Between Dissolved Fe(II) and P

Dissolved P and Fe(II) were significantly ($p < 0.01$) correlated from 0 to 0.008 g boehmite ($R = 0.88$, 0.73, 0.90, and 0.87 for the 0, 0.002, 0.004, and 0.008 g boehmite systems respectively), suggesting that reductive P dissolution from ferrihydrite occurred. Non-significant ($p > 0.05$) correlations between Fe(II) and P were observed for the 0.02 through 0.7 g systems.

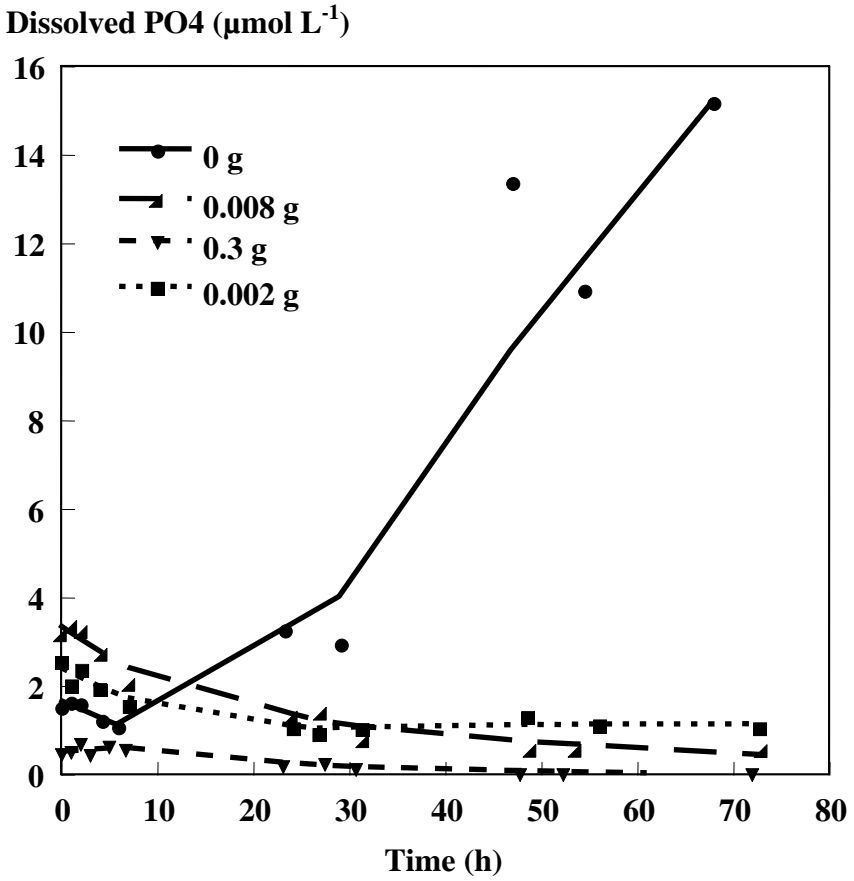

Figure 2.8. Trends in dissolved PO_4 over time for Selected 72-h mixed mineral redox reactor experiments with 0.5 g ferrihydrite, 0, 0.002, 0.008 and 0.3 g boehmite, and 750 mmol P kg^{-1} solids. Curves are shown for display purposes and do not represent an actual data fit.

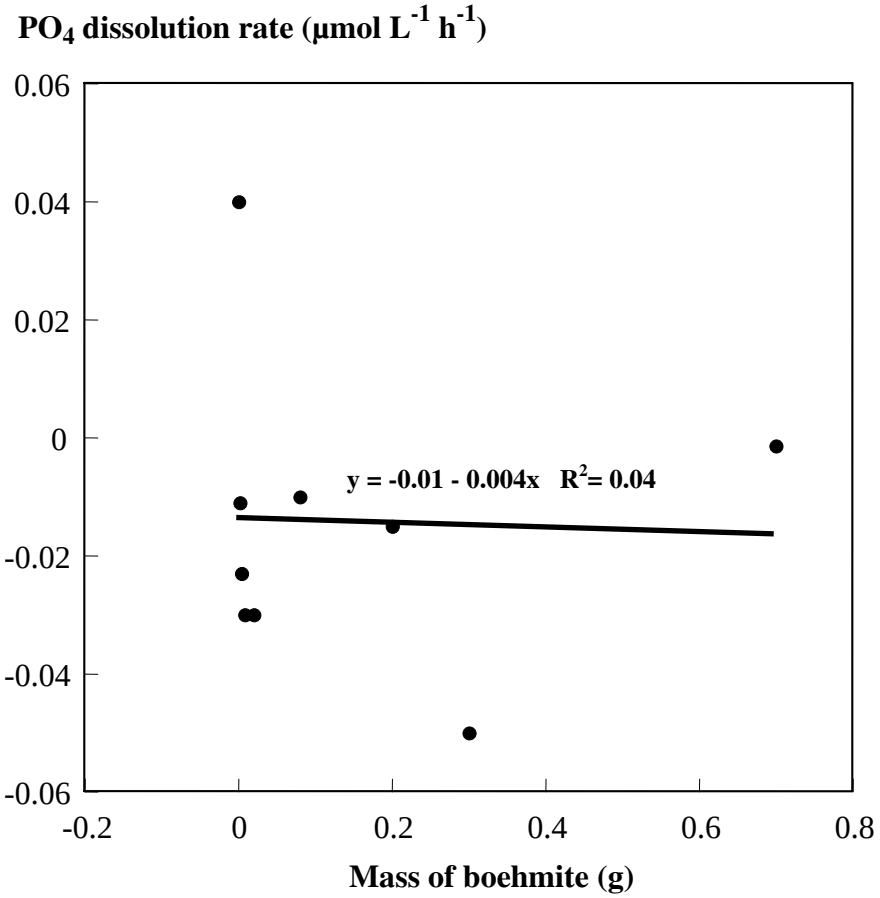

Figure 2.9. Trends in uptake rate coefficients of first order kinetic models fit to dissolved P data for mixed mineral systems with 0.5 g ferrihydrite, 0.002 to 0.7 g boehmite, and 750 mmol P kg^{-1} solids.

Acid Addition Rate

The reduction of iron oxide with H_2 gas can be described by the following reaction (Sposito, 1989):

	Log K	
$1/2H_2(g) \Leftrightarrow H^+(aq) + e^-(aq)$	0.0	(1)
$Fe(OH)_3(s) + 3H^+(aq) + e^-(aq) \Leftrightarrow Fe^{2+}(aq) + 3H_2O(l)$	16.4	(2)
$1/2H_2(g) + Fe(OH)_3(s) + 2H^+(aq) \Leftrightarrow Fe^{2+}(aq) + 3H_2O(l)$	16.4	(3)

Reaction (3) shows that 2 moles of H^+ are consumed for every mole of $Fe(OH)_3$ dissolved. Therefore, the amount of 0.01 M HCl added to each of the reactor systems to maintain a constant pH of 6.0 during 72 h of reduction provides an additional means for quantifying the rate of reactivity in these dissolution experiments.

The amount of acid added as a function of time for selected ferrihydrite/boehmite systems is shown in Figure 2.10. Acid additions were greatest in the 0 g boehmite system and decreased with added boehmite, suggesting that boehmite inhibited the reductive dissolution of Fe oxide. Data were normalized by dividing the amount of acid added by the amount of calculated solids remaining (based on the suspension solids concentration) for each mixed-mineral system. Significant ($p < 0.01$) increases in acid addition over time were observed in all nine experiments. With increasing additions of boehmite, the rate of acid addition decreased. Rate coefficients for zero order kinetic models fit to these data (Figure 2.11) tended to decrease linearly ($R^2 = 0.60$) with increases in boehmite to 0.008 g, analogous to the trends in ferrous iron dissolution rate. A linear relationship between the rate of acid addition and added boehmite was also seen from 0.02 to 0.7 g (Figure 2.11). Neither of these linear relationships were statistically significant, likely due to a small number of data points in the models as noted above.

Equation 3 shows two moles of H^+ being consumed for every mole of Fe(II) dissolved, thereby requiring the addition of two moles of H^+ to maintain a constant pH. Slopes of linear regression models for dissolved Fe as a function of acid added in the redox reactor systems would therefore be expected to have a slope of 0.5 if reductive dissolution solely involved reaction (3). Regression slopes of dissolved iron on acid added for each mixed mineral system appear in Table 2.4 (regression models shown in Figure A.6). Slopes of regression lines for the 0 to 0.008 g systems were $\geq$ 0.5, while all other systems exhibited regression slopes < 0.1. Furthermore, dissolved ferrous iron and acid added were significantly ($p < 0.01$) correlated from 0 to 0.008 g boehmite, but not in the 0.02 to 0.7 g systems, suggesting that a chemical mechanism other than ferrihydrite dissolution caused a consumption of protons in the latter systems. Following are discussions of other possible reaction mechanisms involved in these reduction experiments.

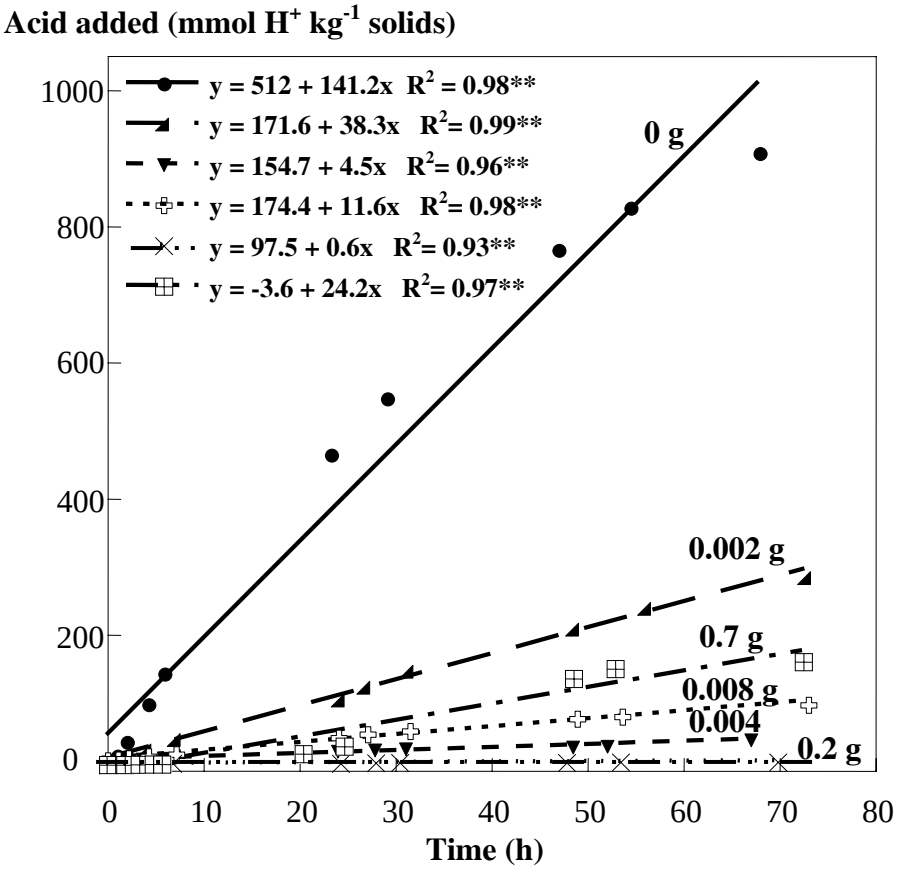

Figure 2.10. Acid (0.01 M HCl) inputs needed to maintain pH 6.0 for selected ferrihydrite - boehmite reactor systems with 0.5 g ferrihydrite, 0 to 0.2 g boehmite, and 750 mmol P kg^{-1} solids. **$p < 0.01$

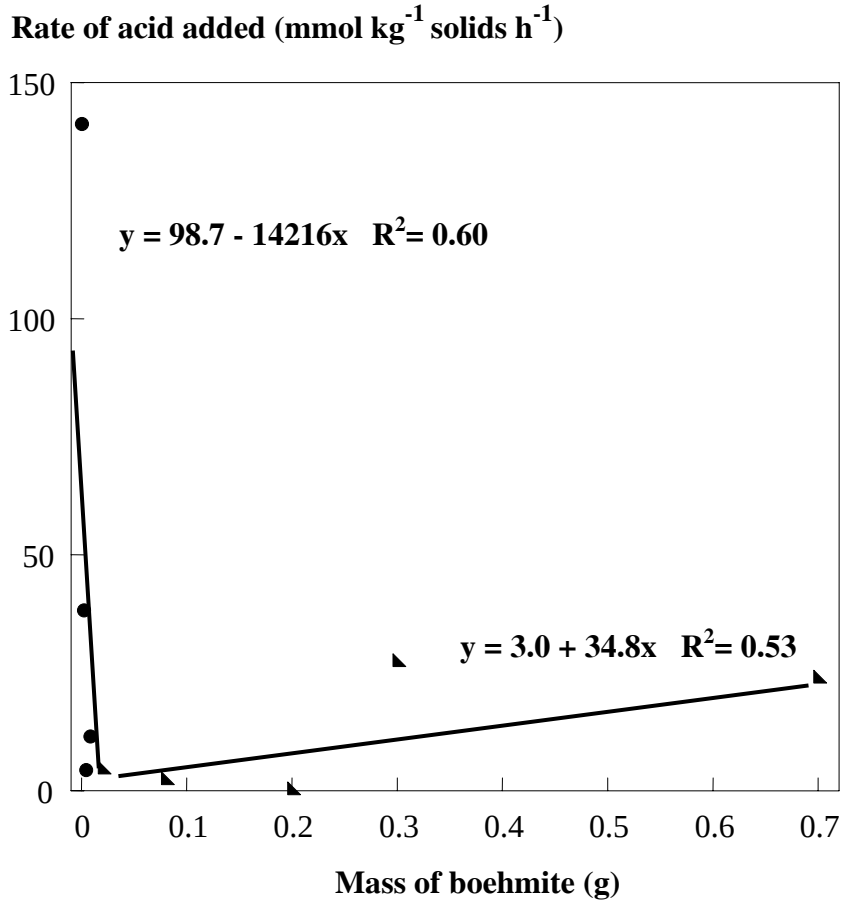

Figure 2.11. Trends in the rate of acid addition (normalized for remaining mineral in suspension) as a function of added boehmite for mixed mineral reactor systems with 0.5 g ferrihydrite, 0 to 0.7 g boehmite, and 750 mmol P kg^{-1} solids.

Table 2.4. Slopes of regression models for dissolved Fe(II) and acid added in systems with 750 mmol P kg^{-1} solids, 0.5 g ferrihydrite, and 0 to 0.7 g boehmite.

Mass of boehmite (g)	Slope of Linear Model	Correlation Coefficient
0	0.57	0.98**
0.002	0.52	0.98**
0.004	1.8	0.92**
0.008	0.2	0.94**
0.02	0.08	0.18
0.08	0.02	0.27
0.2	0.04	0.02
0.3	0.004	0.1
0.7	0.001	0.03

****p < 0.01**

Supporting Experiments

Increasing additions of boehmite in mixed ferrihydrite/ boehmite systems decreased the rate of ferrous iron dissolution between 0 and 0.008 g boehmite, and dissolution rates near zero were observed between 0.02 and 0.7 g boehmite. Dissolved phosphate decreased during reduction in systems containing boehmite. To help explain these trends, several additional experiments were conducted. These auxiliary experiments were designed to investigate three potential mechanisms that may explain the inhibition of ferrihydrite dissolution by boehmite, and the decrease in dissolved phosphate. These mechanisms were:

1) The release of dissolved ferrous iron and phosphate from ferrihydrite and subsequent uptake by boehmite.

2) Inhibition of ferrihydrite dissolution by sorption of Al(III) dissolved from boehmite.

3) Inhibition of dissolution due to inactivation of the 10 % Pt on C catalyst by Al(III) sorption.

Data from each of these supporting experiments is presented below.

1). The release of dissolved ferrous iron and phosphate from ferrihydrite and subsequent uptake by boehmite.

Ferrous iron

Figure 2.12 shows an adsorption isotherm for ferrous iron sorbed to boehmite. A Freundlich sorption model fit to the isotherm data reveals a maximum Fe(II) sorption capacity > 200 mmol Fe(II) kg^{-1}. To account for the difference in dissolved Fe(II) between the 0 and 0.7 g boehmite experiments (decrease in maximum dissolved Fe(II) from 2,000 to 5 μmol L^{-1}), this 0,7 g of boehmite would need to possess a Fe(II) sorption capacity of greater than 2,850 mmol Fe(II) kg^{-1}; more than 10 fold greater than what was observed.

Phosphate

XANES data from a 168-h solid phase redox reactor experiment are shown in Figure 2.13 a. The energy scale is relative to 2149 eV, based on calibration to a variscite spectrum. Khare et al., (2004) showed a distinct pre-edge feature in the spectrum of P sorbed to ferrihydrite that is lacking in the spectra of P bound to boehmite. Pre-edge features of the overall data spectrum are shown in Figure 2.13 b. The spectra from each temporal sample match that of ferrihydrite, and do not exhibit features indicative of boehmite during reduction.

Least squares linear combination fitting (Hutchison et al., 2001, Khare et al., 2004) was utilized to quantitatively compare spectra for samples collected over 168 h to standards of P sorbed to ferrihydrite and boehmite. The results of this fitting are shown

in Table 2.5. Regression analysis of the association of P with ferrihydrite and boehmite over time showed no significant trend in P association with either of these minerals (Figure A.7). These results suggest that P was not reductively dissolved from ferrihydrite and scavenged by boehmite in this particular system.

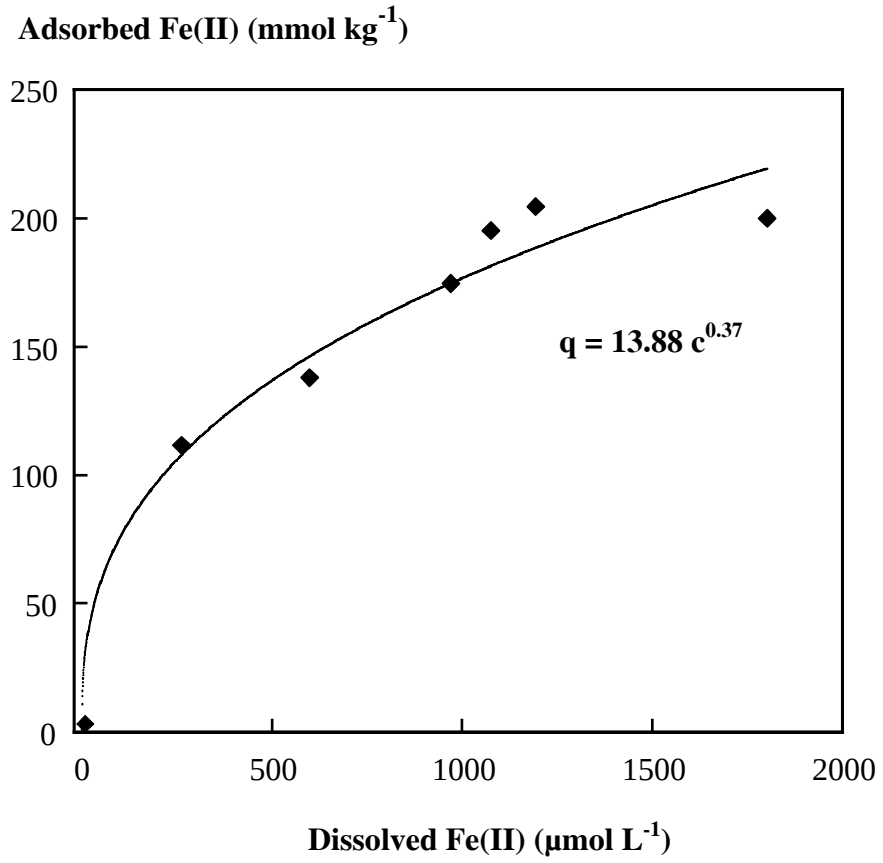

Figure 2.12. Adsorption isotherm for Fe(II) on boehmite. The smooth curve is a Freundlich model fit to the data. Experimental procedures were conducted in an N_2-purged glovebox to inhibit oxidation of ferrous iron.

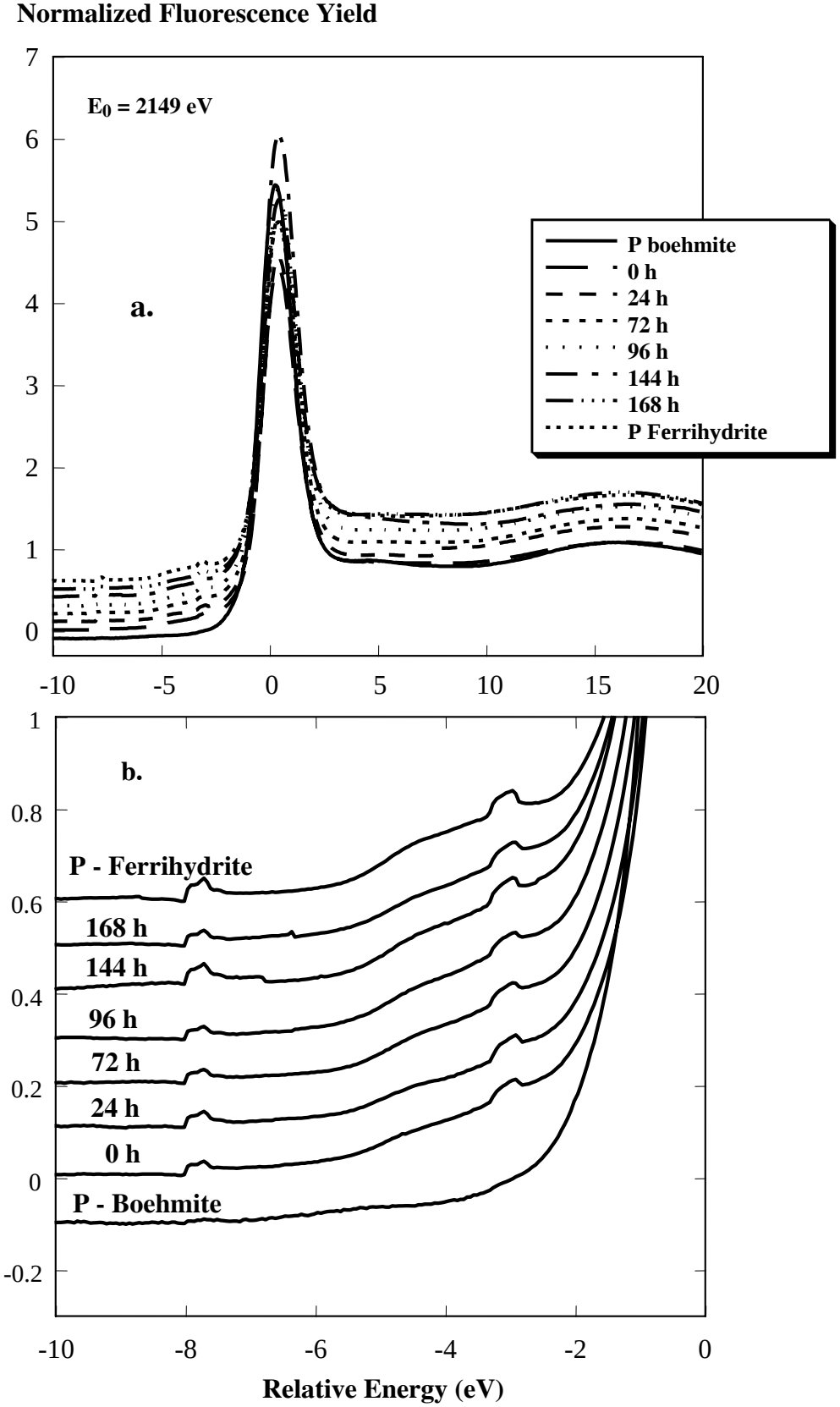

Figure 2.13. Phosphorus K-XANES spectra (a) and pre-edge region of spectra (b) for 168 h 1:1 by mass ferrihydrite:boehmite redox reactor experiment with 750 mmol P kg^{-1} solids. Standards of PO4 adsorbed on boehmite (500 mmol kg^{-1}) and ferrihydrite (1000 mmol kg^{-1}) are included.

Table 2.5. Linear combination fitting results for XANES spectra collected over a 168 h reduction experiment. Data were fit with 1000 mmol P kg^{-1} on ferrihydrite and 500 and P kg^{-1} boehmite to determine the fraction of total P in each sample represented by P sorbed to ferrihydrite or boehmite.

Sample	P - Ferrihydrite* (%)	P- Boehmite* (%)	χ^2
0 h	68 ± 1	32 ± 7	0.006
24 h	53 ± 2	47 ± 7	0.009
72 h	61 ± 1	39 ± 4	0.004
96 h	56 ± 1	44 ± 4	0.004
144 h	75 ± 2	25 ± 12	0.03
168 h	70 ± 1	30 ± 9	0.007

*Standard errors and χ^2 values computed with KaleidaGraph software

2). Inhibition of ferrihydrite dissolution by Al(III) dissolved from boehmite.

Quantification of dissolved Al(III) in a 30 mL subsample of boehmite stock suspension revealed 320 µmol L^{-1} of Al(III) at pH 6.2. Experiments assessing the effect of dissolved Al on reductive ferrihydrite dissolution were therefore performed. Trends in ferrous iron dissolution for systems with inputs of 0, 66.5, 267 and 2,667 mmol Al(III) per kg of ferrihydrite added at pH 3.0 (inputs analogous to the amounts (in mmol) of Al(III) in mixed-mineral suspensions containing 0, 0.002, 0.008 and 0.08 g boehmite, assuming complete dissolution) are shown in Figure 2.14. A decrease in dissolved ferrous iron with increasing pre-sorbed Al(III) was observed in these systems (maximum Fe(II) after 48 h of reduction approximately 350, 300, 150 and 0 µmol L^{-1} for the 0, 66.5, 266.7 and 2,666.7 mmol Al(III) kg^{-1} systems respectively). The lowest of these three inputs was below the Al(III) sorption capacity for ferrihydrite quantified in the 2,667 mmol Al(III) input system (430 mmol kg^{-1}). Significant ($p < 0.01$) correlations between dissolved Fe(II) and time were found for the 0 to 267 mmol Al(III) systems, and Fe(II) and Al(III)

input were correlated (R = 0.85), but not statistically significant (correlation models not shown).

Data from a control experiment consisting of 0 moles of Al(III) added to ferrihydrite at pH 6.0 performed within two weeks of the Al(III) sorption experiments is also presented in Figure 2.14. The maximum dissolved Fe(II) after 48 hours of reduction was 715 μmol L^{-1} in this system as compared to 350 μmol L^{-1} for the pH 3.0 system.

Statistical comparison of the rate of Fe(II) dissolution in the sorbed Al(III) systems revealed no significant differences among the 0, 67, 267, and 2,667 mmol Al(III) kg^{-1} systems. Additionally, the rate of Fe(II) dissolution was not statistically different between the 0 mmol Al(III) pH 3.0 and 6.0 systems. Comparison of the rate of Fe(II) dissolution between the 0, 67, 267 and 2,667 mmol Al(III) from boehmite reactor systems and the analogous Al(III) from $AlCl_3$ systems revealed no significant differences ($p > 0.05$), suggesting that the decrease in dissolved Fe(II) in reactor systems containing from 0 to 0.008 g boehmite may be attributed to sorption of Al(III) to the ferrihydrite surface.

3). Inhibition of dissolution due to Al(III) sorption on 10 % Pt on C catalyst.

A 24 hour sorption experiment with 266 mmol Al(III) kg^{-1} (the calculated amount of Al(III) that could potentially be sorbed to 0.125 g 10 % Pt on activated C catalyst assuming complete dissolution of 0.008 g boehmite) equilibrated on 10% Pt on activated C catalyst revealed that the catalyst sorbed 186 mmol Al(III) kg^{-1}. The dissolved Fe(II) data from a 48-h redox reactor experiment utilizing the above mentioned Al(III) equilibrated catalyst appears in Figure 2.15. This figure also shows the trend in dissolved Fe(II) in the absence of Al(III) sorbed to 10% Pt on activated C catalyst. While there was an apparent difference in dissolution rate for the catalysts with and without sorbed Al (slopes of the linear models were 6.2 and 15.8 for the systems with catalysts containing 266 mmol Al(III) sorbed and no sorbed Al(III), respectively), these rates were not significantly different at the $\alpha = 0.05$ probability level.

The input of Al(III) in the catalyst suspension was greater than the actual proportion of Al(III) sorbed, meaning that 20 mmol dissolved Al(III) kg^{-1} ferrihydrite was added to the reactor system with this catalyst suspension. Figure 2.14 compares the Fe(II) dissolution data from this experiment with the $AlCl_3$ reactor experiments discussed above. The dissolution trend for this system falls between those for the 0 and 67 mmol Al(III) kg^{-1} systems.

An additional experiment with Al(III) added at a rate of 130 mmol kg^{-1} (below the threshold Al sorption capacity of 186 mmol kg^{-1} for 10 % Pt on activated C catalyst) showed an apparent suppression of Fe(II) dissolution in the system with Al(III) sorbed to the catalyst, suggesting that catalyst deactivation may help to explain the

decreases in dissolved Fe(II) with increasing boehmite in the core reactor experiments (Figure A.9).

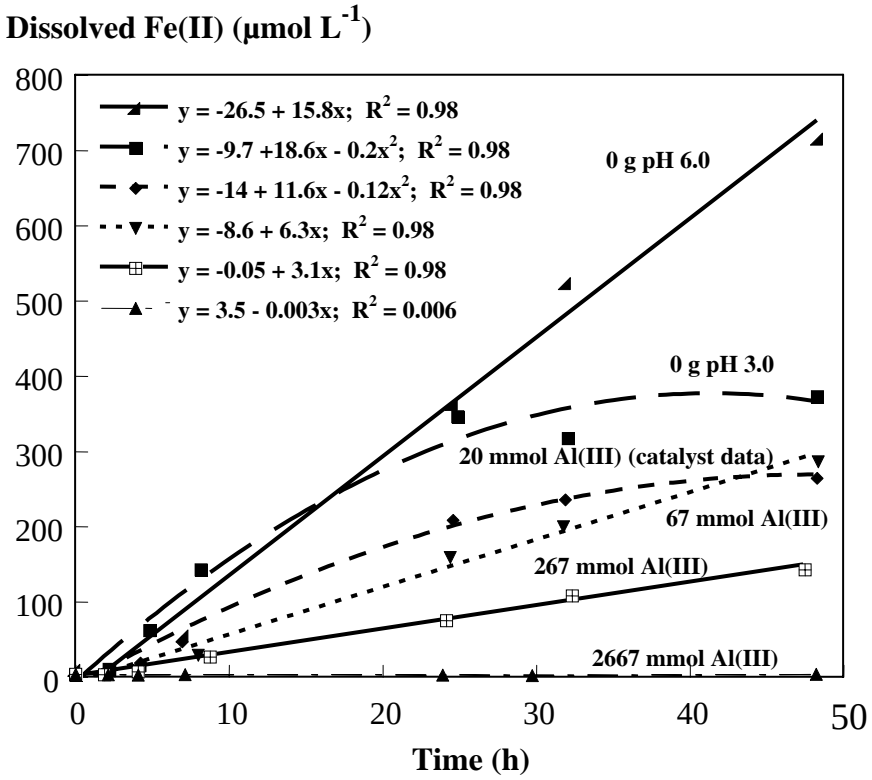

Figure 2.14. Trends in dissolved Fe(II) for redox reactor systems containing ferrihydrite and the equivalent moles Al(III) in 0, 0.002, 0.008 and 0.08 g boehmite (0 to 2,667 mmol Al(III) kg^{-1} respectively) at pH 6.0 .

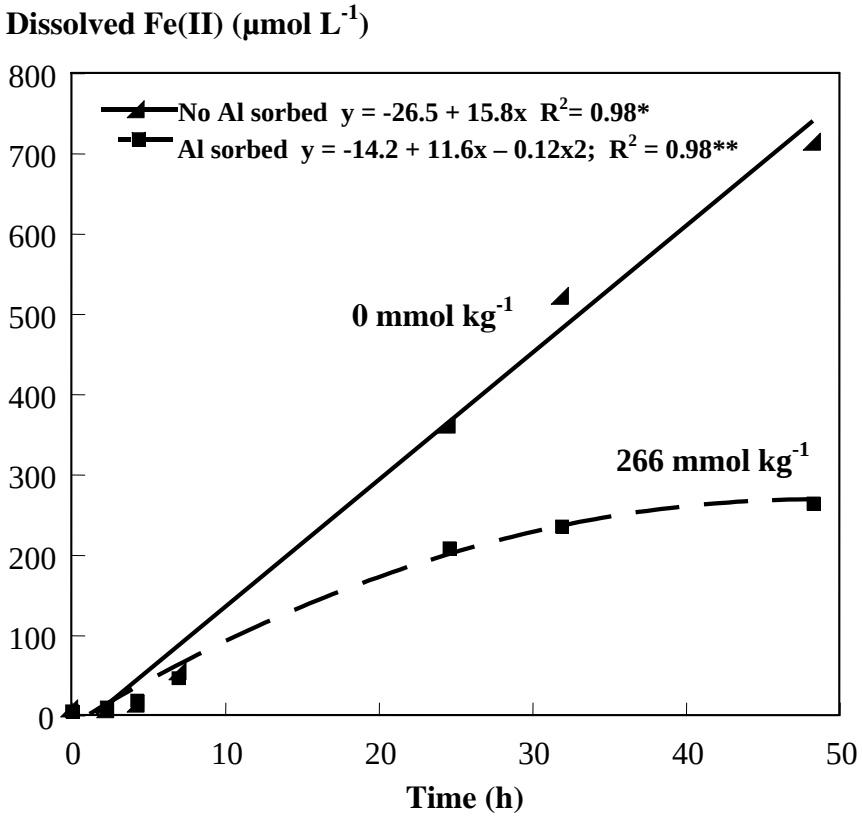

Figure 2.15. Trends in dissolved Fe(II) for redox reactor systems with 0 or 266 mmol Al kg^{-1} sorbed on 10 % Pt on activated carbon catalyst. **$p < 0.01$

DISCUSSION

The addition of 0.002 g of boehmite to a mixed ferrihydrite – boehmite reactor system caused a sharp decrease in the rate of Fe(II) dissolution. The dissolution rate decreased linearly between 0 and 0.008 g of added boehmite, and was essentially zero from 0.02 to 0.7 g of boehmite. Dissolved phosphate decreased during reduction in all boehmite-containing systems, and exhibited rates of uptake that were independent of added boehmite. Evaluation of the acid added in reactor systems with boehmite inputs above 0.008 g showed less net H^+ added as compared to the 0 to 0.008 g systems. However, the proton additions in these systems were greater than those expected considering ferrihydrite dissolution exclusively (i.e., ratio of dissolved Fe(II)/ added H^+ < 0.5), suggesting that another chemical reaction was responsible for the consumption of protons. Table 2.6 lists possible reactions that could control the addition of protons in the ferrihydrite/boehmite reactor systems. Of the reactions listed, only reductive dissolution of ferrihydrite and boehmite dissolution (to $Al^{3+}_{(aq)}$) resulted in a net consumption of protons.

To explain the above results, four possible mechanisms were considered. These mechanisms were the scavenging of reductively dissolved Fe(II) and P by boehmite, the inhibition of ferrihydrite reduction from sorbed Al(III), the deactivation of 10% Pt on activated carbon catalyst by sorbed Al(III), and the formation of Fe- or Al- phosphate minerals.

Due to the stability of Al-oxides under reduced soil conditions, one could expect these minerals to serve as scavengers of reductively dissolved Fe(II) and P. For example, associations of P with Al-oxide minerals in reduced environments have been reported in

Table 2.6. Possible chemical reactions occuring in mixed ferrihydrite-boehmite reduction reactor systems at pH 6.0.

Reaction Number	Reaction	Description
(1)	$1/2H_{2(g)} + Fe(OH)_{3(s)} + 2H^{+}_{(aq)} \Leftrightarrow Fe^{2+}_{(aq)} + 3H_2O_{(l)}$	Reductive dissolution of Fe-oxide
(2)	α-$AlOOH_{(s)} + 3H^{+}_{(aq)} \Leftrightarrow Al^{3+}_{(aq)} + 2H_2O_{(l)}$	Boehmite dissolution
(3)	$Al^{3+}_{(aq)} + 2H_2O_{(l)} \Leftrightarrow Al(OH)_2^{+}{}_{(aq)} + 2H^{+}_{(aq)}$	Aluminum hydrolysis[a]
(4)	$Al^{3+}_{(aq)} + 2H_2O_{(l)} \Leftrightarrow Al(OH)_2^{+}{}_{(aq)} + 2H^{+}_{(aq)}$	Aluminum hydrolysis[a]
(5)	$Al^{3+}_{(aq)} + H_2O_{(l)} \Leftrightarrow AlOH^{2+}{}_{(aq)} + H^{+}_{(aq)}$	Aluminum hydrolysis
(6)	$Al^{3+}_{(aq)} + 3H_2O_{(l)} \Leftrightarrow Al(OH)_3^{0}{}_{(aq)} + 3H^{+}_{(aq)}$	Aluminum hydrolysis
(7)	$Fe^{2+}_{(aq)} + 2OH^{-}_{(aq)} \Leftrightarrow Fe(OH)_{2(s)}$	Green rust precipitation
(8)	$Fe^{2+}_{(aq)} >Al\text{-}OH_2^{+}{}_{(s)} \Leftrightarrow >Al\text{-}OFe^{+}_{(s)} + 2H^{+}(aq)$	Fe(II) sorption on boehmite.; $PZC_{boe.} = 8.2$[b]
(9)	$3Fe^{2+}_{(aq)} + 2H_2PO_4^{-}{}_{(aq)} + 8H_2O_{(l)} \Leftrightarrow Fe_3(PO_4)_2{\cdot}8H_2O_{(s)} + 4H^{+}_{(aq)}$	Vivianite precipitation
(10)	$Fe\text{-}OPO_3H_{2(s)}^{(+2)} + 1/2H_{2(g)} \Leftrightarrow H^{+}_{(aq)} + Fe^{2+}_{(aq)} + H_2PO_4^{-}{}_{(aq)}$	Reductive P dissolution from ferrihydrite
(11)	$H_2PO_4^{-}{}_{(aq)} + >Al\text{-}OH_2^{+}{}_{(s)} \Leftrightarrow >Al\text{-}OPO_3H_{2(s)} + H_2O_{(aq)}$	P adsorption to boehmite
(12)	$Al(OH)_2^{+}{}_{(aq)} + >Fe\text{-}OH_2^{+}{}_{(s)} \Leftrightarrow >Fe\text{-}OAl(OH)_{2(s)} + 2H^{+}_{(aq)}$	Al(III) sorption to ferrihydrite; $PZC_{ferri.} = 8.5$[b]
(13)	$Al^{3+}_{(aq)} + H_2PO_4^{-}{}_{(aq)} + 2H_2O(l) \Leftrightarrow AlPO_4{\cdot}2H_2O_{(s)} + 2H^{+}_{(aq)}$	Variscite precipitation
(14)	$Fe^{2+}_{(aq)} + H_2PO_4^{-}{}_{(aq)} \Leftrightarrow FeH_2PO_4^{+}{}_{(aq)}$	Fe(II) - P aqueous complex

[a]Dominant Al hydrolysis species at pH 6.0
[b]McBride, 1994

the literature (Richardson, 1985, Axt and Walbridge, 1999). However, the maximum sorption capacity of boehmite for ferrous iron (225 mmol kg^{-1}, Figure 2.12) is approximately ten fold less than that needed to account for a difference of 2,850 µmol Fe(II) L^{-1} observed between the 0 and 0.7 g boehmite systems. Additionally, the maximum sorption capacity of the mineral mixture (308 mmol kg^{-1} total) containing 0.5 g ferrihydrite (Fe(II) sorption capacity of 300 mmol kg^{-1}, data not shown) and 0.7 g boehmite (Fe(II) sorption capacity of 225 mmol kg^{-1}) is also not sufficient to explain the loss of ferrous iron in solution between the 0 and 0.7 g systems.

The observed uptake of P over time in the reduction reactor systems could potentially be explained by the scavenging of dissolved P by boehmite. Sorption of PO_4 on oxide minerals continues to increase at times greater than 24 hours (van Riemsdijk and Lyklema, 1980). To explain the decrease in maximum dissolved phosphate from 15 µmol L^{-1} in the 0 g boehmite system to essentially 0 µmol L^{-1} in the 0.7 g boehmite system based on the ability of boehmite to scavenge P, a maximum P sorption of 21 mmol kg^{-1} is necessary. The actual P sorption capacity of boehmite is 600 mmol kg^{-1}, which is 30-fold greater. However, this sufficiency in P sorption capacity of boehmite does not necessarily explain a temporal trend in P uptake during reduction. For example, the 0.6 µmol potential P sorption capacity of 0.002 g boehmite is three fold less than the 1.8 µmol P (difference in dissolved P at 0 and 30 h for the 0.002 g boehmite system) that is uptaken in this system. Furthermore, substantial portions of the boehmite solids are expected to dissolve as described above.

The distribution of P among ferrihydrite and boehmite showed a trend of decreasing P associated with Al(III) rather than Fe(II) during 168 h of reduction in the

solid phase P speciation experiment (Table 2.5, Figure A.7), the linear regression was not significant ($p > 0.05$).

Previous work has shown phosphate at concentrations near 750 mmol P kg^{-1} to be distributed between Fe- and Al-oxides in direct proportion to each mineral's contribution to the overall P sorption capacity of the system (Khare et al., 2004). Consequently, P would be distributed in this system at 68 and 32 % for ferrihydrite and boehmite, respectively, based on the maximum sorption capacity of these minerals at the time of this experiment. This predicted distribution is the same as that found after P equilibration with ferrihydrite and boehmite for 24 h in the reduction reactor system (0 h of reduction, Table 2.5), suggesting that our data were consistent with those of Khare et al., (2004).

We conclude that a net transfer of P between ferrihydrite and boehmite was not detected by XANES analysis in this particular experiment. It should be noted that the loss of dissolved P between the 0 and 0.7 g boehmite systems (12.5 mmol kg^{-1}, assuming boehmite scavenging) would not be detected above experimental error by XANES analysis (a 2% change in distribution) relative to an estimated XANES detection limit of approximately 10 % change.

Because of the apparent loss of dissolved P over time in the presence of boehmite, and the lack of boehmite P sorption capacity necessary to explain uptake in these systems, we hypothesize the formation of ferrihydrite-PO_4-Al-PO_4 surface complexes or precipitates in these ferrihydrite/boehmite mixtures, analogous to goethite-PO_4-Fe(III)-PO_4 surface precipitates proposed by Ler and Stanforth (2003). The formation of ternary surface complexes involving Cu and PO_4 bound to Al-oxide surfaces has been shown (Clark and McBride, 1985).

The boehmite used in the redox reactor experiments is poorly crystalline, and has a correspondingly high surface area (514 m^2 g^{-1}, measured by H_2O adsorption, Wang et al., 2002). Consequently, boehmite in the mixed mineral systems could be expected to contribute dissolved Al(III), which can subsequently be sorbed on ferrihydrite. In addition, we measured 320 µmol Al(III) L^{-1} in a subsample of our boehmite stock suspension at pH 6.2 which had been stored at 4°C for 450 d. The lack of detectable Al in the reduction reactor experiments at pH 6.0 supports the conjecture that Al dissolved from boehmite would be sorbed on ferrihydrite. This dissolution of poorly crystalline Al-oxide would be expected to consume three moles of H^+ for every mole of boehmite dissolved according to Reaction 2 in Table 2.6. Considering the relative activities of Al hydrolysis species at pH 6 (60% $Al(OH)^{2+}$, 20% $Al(OH)_4^-$, 10% $Al(OH)_3^0$ and 8% $AlOH^{2+}$, Lindsay, 1979), Al^{3+} hydrolysis should generate 2-4 mol H^+ per mol $Al^{3+}{}_{(aq)}$. Thus the overall net consumption of protons from boehmite dissolution and Al hydrolysis should be 0.6 (combining reaction 2 with reactions 3 to 6 in table 2.6). Consequently, these reactions provide support for the greater addition of H^+ relative to Fe(II) dissolution for systems containing boehmite.

Decreases in the reductive dissolution of iron oxide have been observed with increases in Al substitution (Gonzalez et al., 2002). Certain authors have hypothesized the formation of non-reducible Al coatings precipitated at the Fe-oxide surface, which inhibit reductive dissolution (Segal and Sellers, 1984, Bousserrhine et al., 1998). The sorption of Al(III) on ferrihydrite may also inhibit reductive dissolution by blocking electron transfer to the iron oxide surface. Furthermore, ferrihydrite demonstrated the

ability to sorb Al(III) (up to 430 mmol kg^{-1} ferrihydrite at an Al(III) input of 2,667 mmol kg^{-1} at pH 3.0).

The Al(III) present in mixed systems (assuming complete boehmite dissolution) plotted as a function of Fe(II) dissolution rate (Figure A.8) produces trends similar to those observed for ferrous iron dissolution as a function of added boehmite (Figure 2.7). These similarities suggest that the trends in the decreased rate of ferrous iron dissolution with added boehmite could be attributed to Al(III) surface coverage as described above. While the sorption of Al(III) to ferrihydrite could be expected to generate 2 moles of H^+, thereby offsetting the mole of H^+ consumed by boehmite dissolution and Al^{3+} hydrolysis (Reactions 2,3, 4 and 11; Table 2.6), the bonding mechanism of Al(III) on the ferrihydrite surface in our systems is not known. Therefore, the deviation of expected H^+ to Fe(II) stoichometry in the higher boehmite systems may still be the consequence of boehmite dissolution and subsequent Al(III) sorption on ferrihydrite.

The use of platinum on activated carbon catalyst has been documented for iron oxide reduction experiments (Williams and Patrick, 1971, Willet and Cunningham, 1983, Brennan and Lindsay, 1998). This material enhances the transfer of electrons present during abiotic reduction by adsorbing H_2, which in turn becomes an electron source to the metal oxide (Barbier et al., 1996). These electron transfer characteristics are further enhanced by a high surface area (500 to 1500 $m^2\ g^{-1}$) activated carbon carrier, which further enhances the reactivity of the platinum metal (Grove, 2002). Catalyst "poisoning" or the deactivation of catalytic material from the sorption of metal species to the active surface sites is documented in the catalyst literature (Sivasanker, 2002). Dissolved aluminum sorbed to the catalyst surface could potentially decrease catalytic activity.

Data from the Al(III) sorbed catalyst redox reactor experiments help support this hypothesis, showing an observed decrease in reductive ferrihydrite dissolution rate for the system with Al(III) pre-sorbed on the catalyst (Figure 2.15). This mechanism may help to explain the linear decrease in Fe(II) dissolution rate with increasing additions of boehmite, particularly in systems with relatively low sorbed Al(III) compared to the sorption maximum for ferrihydrite (the 0.002 to 0.008 g systems). It should be noted that 20 mmol dissolved Al(III) kg^{-1} ferrihydrite was added with the Al(III) sorbed catalyst suspension in this experiment because of $AlCl_3$ added in excess of the catalyst sorption capacity. The fact that Fe(II) dissolution for this experiment lies between that of the 0 and 67 mmol Al(III) systems provides evidence that the decreased Fe(II) dissolution in this solution came from surface coverage of Al(III) on ferrihydrite, and not from an inhibition of Pt catalyst. However, the analogous experiment conducted approximately 40 days later with Al(III) added below the maximum Al sorption capacity of platinum catalyst (Figure A.9) provides compelling evidence that catalytic deactivation from dissolved Al(III) may have occurred in the reduction reactor experiments. It should be noted that we do not know whether Al was transferred from the catalyst to the ferrihydrite (of greater Al sorption capacity) when the two materials were mixed.

The precipitation of an iron or aluminum phosphate mineral would result in loss of P from solution during reduction in the mixed mineral systems. These minerals would be expected to form if the system was supersaturated with respect to that particular mineral. The precipitation of variscite, an aluminum phosphate mineral, is described by Reaction 13 of Table 2.6. This reaction would generate protons, and the observed addition of H^+ would therefore not be seen if this reaction were a dominant pH-dependent

reaction. The formation of vivianite, a ferrous iron phosphate mineral is given by Reaction 9 of Table 2.6. Again, precipitation of this mineral would generate protons, thereby requiring the addition of OH^- rather than H^+. Furthermore, we would also expect to see a change in P K-XANES spectra if vivianite formed in the supporting spectroscopy experiment, based on XANES data for a vivianite standard. Based on proton addition trends and XANES analysis, we discount the formation of iron and aluminum phosphate minerals as a less significant mechanism for P uptake than the sorption of dissolved P from Al(III) dissolved from boehmite as described above.

In summary, results from the supporting experiments evaluating the role of boehmite as an Fe(II) and P scavenger, the inhibition of ferrihydrite reduction and catalytic activity from Al(III) dissolved from boehmite, and the formation of Al or Fe phosphate minerals suggests that boehmite inhibited Fe-oxide reductive dissolution in mixed Fe- and Al-oxide mineral systems. Additionally, the net P in solution decreased over time in these systems. The proposed mechanisms are the partial dissolution of boehmite resulting in Al(III) which blocks electron transfer to the ferrihydrite surface, and the uptake of P during reduction by boehmite.

Implications of this Research for Soil P Management

Soils are inherently complex, consisting of primary and secondary minerals, organic materials, and a multitude of microorganisms. This complexity makes the understanding of the basic chemistry behind reductive dissolution of phosphate difficult. The study of relevant processes in pure mineral systems is desirable for understanding

fundamental abiotic chemical reactions that serve as a basis for research on more complex biotic redox reactions in soils.

The goal of this research was to understand the specific roles of iron and aluminum oxides in reductive P dissolution. These minerals are considered the most important constituents for retaining soil P. Dissolved P appeared to be taken up by boehmite in our mixed-mineral reactor systems. However, a more pronounced effect of boehmite addition to the mineral mixtures was the inhibition of ferrihydrite reduction, likely from Al-oxide dissolution and Al(III) sorption on ferrihydrite which inhibited electron transfer to Fe(III) in the iron oxide mineral. Our results suggest that dissolved P in reduced soils containing poorly crystalline iron and aluminum oxide minerals may be uptaken by non-redox active Al-oxide minerals. Additionally, P sorbed to iron oxides may be inhibited from dissolution due to the effects of dissolved Al(III) bound to the iron oxide surface, although this result would be less applicable if dissolved Al(III) were bound to organic matter or other metal adsorbing constituents common to soils.

In the initial phases of experimentation, it was concluded that ferrihydrite reduction could not be accomplished in the absence of a platinum catalyst. Our findings underscore the importance of soil microbes in catalyzing redox reactions in soils by providing biotic mechanisms that transfer electrons between reducing agents such as organic C and electron acceptors such as Fe(III)-oxides. The importance of soil organic matter in enhancing P dissolution has been shown in the literature (Hutchison and Hesterberg, 2004), and the majority of reductive P dissolution studies have utilized biotic reduction, which depends on soil microbes and organic matter (Sallade and Sims, 1997, Young and Ross, 2001).

CONCLUSIONS

Our studies on abiotic reduction of phosphated ferrihydrite in physical mixtures of ferrihydrite and boehmite at pH 6.0 showed that additions of boehmite up to 0.008 g kg^{-1} suspension (0.5 g kg^{-1} ferrihydrite) caused linear ($R^2 = 0.61$) decreases in zero-order rate coefficients for Fe(II) dissolution. Ferrihydrite dissolution rates were essentially zero between 0.02 and 0.7 g kg^{-1} added boehmite. Dissolved phosphate decreased during reduction of systems containing boehmite, indicating that P was sorbed as reduction progressed. No significant trend between P uptake rate and increasing boehmite was observed, suggesting that P was sorbed at a similar rate in all systems regardless of added boehmite. The observed stoichiometric relationship among dissolved Fe(II) and acid added to maintain a constant pH of 6.0 in the reactor systems revealed that acid was added in excess of what would be expected for ferrihydrite dissolution in the presence of 0.02 to 0.7 g kg^{-1} added boehmite, suggesting that another chemical mechanism was responsible for the consumption of protons.

Supporting experiments evaluated the potential scavenging of dissolved Fe(II) and P by boehmite, the inhibition of ferrihydrite reduction due to Al(III) sorbed to either the surface of the ferrihydrite or the Pt catalyst, and the formation of Fe- or Al- phosphate minerals. Boehmite lacked the sorption capacity to account for the loss of dissolved Fe(II) observed for added boehmite between 0 and 0.7 g kg^{-1} suspension. A solid phase P speciation experiment using P K-XANES analysis detected no net transfer of PO_4 between ferrihydrite and boehmite. Reactor experiments with dissolved Al(III) showed decreased rates in ferrous iron dissolution with increasing Al(III). Based on these findings and expected relationships among proton stoichometry, the inhibition of

ferrihydrite reductive dissolution and uptake of P by Al(III) dissolved from boehmite and sorbed to the surface of ferrihydrite (and perhaps the Pt catalyst) best explained the observed trends.

The results suggest that in the absence of organic matter (e.g., perhaps in low organic matter subsoils), mineralogical surface changes occurring during reduction may enhance the uptake of dissolved PO_4 in soils. Additionally, iron oxide reduction may be inhibited in the presence of poorly crystalline Al-oxides due to sorption of Al(III) on the Fe-oxide.

REFERENCES CITED

Amacher, M.C. 1991. Methods of obtaiing and analyzing kinetic data. pp. 19-59 *In*: D.L. Sparks (Ed.) Rates of soil chemical processes. SSSA Special Publication No. 27. Soil Sci. Sco. Am., Madison, WI.

Axt, J.R. and M. R. Walbridge. 1999. Phosphate Removal Capacity of Palustrine Forested Wetlands and Adjacent Uplands in Virginia. Soil Sci. Soc. Am. J. 63:1019–1031.

Barbier, J., Chollier, M.J., and F. Epron. Catalysis by metals: contribution of electrochemistry. pp. 111-131. In: A.J. Renouprez and H. Jobic (Eds.) Catalysis by Metals. Springer, Paris, France.

Beauchemin, S. and R.R. Simard. 1999. Soil phosphorus saturation degree: Review of some indices and their suitability for P management in Quebec, Canada. Can. J. Soil Sci. 79:615-625.

Bloom, P.R. 1981. Phosphorus adsorption by an aluminum-peat complex. Soil Sci. Soc. Am. J. 45:267-272.

Borggaard, O.K. 1983. The influence of iron oxides on phosphate adsorption by soil. J. Soil Sci. 34:333-341.

Borggaard, O.K., Jorgensen, S.S., Moberg, J.P., and B. Raben-Lange. 1990. Influence of organic matter on phosphate adsorption by aluminum and iron oxides in sandy soils. J. Soil Sci. 41:443-449.

Bousserrhine, N., Gasser, U., Jeanroy, E., and J. Berthelin. 1998. Effect of aluminum substitutoipn on ferri-reducing bacterial acticity and dissolution of goethites. Earth and Planetary Sciences. 326:617-624.

Brennan, E.W. and W.L. Lindsay. 1998. Reduction and Oxidation effect on the solubility and transformation of iron oxides. Soil Sci. Soc. Am. J. 62:930-937.

Collins, J.F. and S.W. Buol. 1970. Effects of fluctuations in the Eh-pH environment on iron and/or manganese equilibria. Soil Sci. 110:111-118.

Cornell, R.M. and W. Schneider. 1989. Formation of goethite from ferrihydrite at physiological pH under the influence of cysteine. Polyhedron. 8:149-155.

Cornell, R.M., Giovanoli, R., and W. Schneider. 1990. Effect of cysteine and manganese on the crystallization of noncrystalline iron(III) hydroxide at pH 8. Clays and Clay Minerals. 38:21-28.

Correll, D.L. 1998. The role of phosphorus in the eutrophication of receiving waters: A review. J. Environ. Qual. 27:261-266.

Clark, C.J. and M.B. McBride. 1985. Adsorption of Cu(II) by allophane as affected by phosphate. Soil Sci. 139:412-421.

Darke, A.K., and M.R. Walbridge. 2000. Al and Fe biogeochemistry in a floodplain forest: Implications for P retention. Biogeochemistry. 51:(1) 1-32.

DeLaune, R.D., Reddy, C.N. and W.H. Patrick, Jr. 1981. Effect of pH and redox potential on concentration of dissolved nutrients in estuarine sediment. J. Environ. Qual. 10:276-279.

Eghball, B., and J.F. Power. 1999. Phosphorus- and Nitrogen-based manure and compost applications: Corn production and soil phosphorus. Soil Sci. Soc. Am. J. 63:895-901.

Freese, D., S.E.A.T.M. Van der Zee, and W.H. Van Riemsdijk. 1992. Comparison of different models for phophate sorption as a function of the iron and aluminum oxides of soils. J. Soil Sci. 43:729-738.

Gerke, J, and R. Hermannn. 1992. Adsorption of orthophosphate to humic-Fe-complexes and to amorphous Fe-oxide. Z. Pflanzenernahr. Bodenk. 155:233-236.

Gonzalez, E., Ballesteros, M.C., and E.H. Rueda. 2002. Reductive dissolution kinetics of Al-substituted goethites. Clays and Clay Min. 50:470-477.

Gotoh, S. and W.H. Patrick Jr. 1974. Transformation of iron in a waterlogged soil as influenced by redox potential and pH. Soil Sci. Soc. Am. Proc. 38:66-71.

Grove, D.E. 2002. Paste or Powder? Platinum Metals Rev., 46(1):48

Hesterberg, D.L., W. Zhou, K.J. Hutchison, S. Beauchemin, and D.E. Sayers. 1999. XAFS study of adsorbed and mineral forms of phosphate. J. Synchrotron Radiat. 6:636-638.

Holford, I.C.R. and W.H. Patrick Jr. 1979. Effects of reduction and pH changes on phosphate sorption and mobility in an acid soil. Soil Sci. Soc. Am. J. 43:292-297.

Husin, A.B., Caldwell, A.G., Mengel, D.B., and F.J. Peterson. 1987. Effects of natural and artificially induced reduction on soil solution phosphorus in rice soils. Plant and Soil. 102:171-175.

Hutchison, K.J., Hesterberg, D.H., and J.W. Chou. 2001. Stability of reduced organic sulfur in humic acid as affected by aeration and pH. Soil Sci. Soc. Am. J. 65:704-709.

Hutchison, K.J. and D. Hesterberg. 2004. Dissolution of phosphate in a phosphorus-enriched ultisol as affected by microbial reduction. J. Environ. Qual. 33:1793-1802.

Khalid, R.A., Patrick, Jr., and R.D. DeLaune. 1977. Phosphorus sorption characteristics of flooded soils. Soil Sci. Soc. Am. J. 41:305-310.

Khare, N., Hesterberg, D., Beauchemin, S., and S. Wang. 2004. XANES Determination of adsorbed phosphate distribution between ferrihydrite and boehmite in mixtures. Soil Sci. Soc. Am. J. 68:460-469.

Lindsay, W.L. 1979. Chemical equilibria in soils. John Wiley and Sons. New York, NY.

Ler, A. and R. Stanforth. 2003. Evidence for surface precipitation of phosphate on goethite. Environ. Sci. Tecnol. 37:2694-2700

Lockaby, B.G. and M.R. Walbridge. 1998. Biogeochemistry. *In*: Messina M.G. and W.H. Conner (Eds) Southern Forested Wetlands (pp 149–172). Lewis Publishers, Boca Raton, FL.

McBride, m. 1994. Environmental Chemistry of Soils. Oxford University Press. New York, NY.

Moore, P.A. Jr., and K.R. Reddy. 1994. Role of Eh and pH on phosphorus geochemistry in sediments of Lake Okeechobee, Florida. J. Environ. Qual. 23:955-964.

Murphy, J. and J.F. Riley. 1962. A modified single solution method for the determination of phosphate in natural waters. Anal. Chim. Acta 27:31-36.

Newville, M. IFEFFIT. http://cars9.uchicag.edu/ifeffit

Olsen, S.R., and L.E. Sommers. 1982. Phosphorus. pp. 403-430. *In* A. Page et al. (ed.) Methods of soil analysis. Part 2. 2nd ed. SSSA, Madison, WI.

Olson, R.V. and R. Ellis, Jr. 1982. Iron. pp. 301-312. *In* A. Page et al. (ed.) Methods of soil analysis. Part 2. 2nd ed. SSSA, Madison, WI.

Pant, H.K., and K.R. Reddy. 2001. Phosphorus sorption characteristics of estuarine sediments under different redox conditions. J. Environ. Qual. 30:1474-1480.

Parfitt R.L. 1989. Phosphate reactions with natural allophane, ferrihydrite and goethite. J. Soil Sci. 40:359–369.

Patrick, W.H., Gotosh, S., and B.G. Williams. 1973. Strengite dissolution in flooded soils and sediments. Science. 179:564-565.

Patrick, W.H., Jr., and R.A. Khalid, 1974. Phosphate release and sorption by soils and sediments: Effects of aerobic and anaerobic conditions. Science 186:53-55.

Richardson, C.J. 1985. Mechanisms controlling phosphorus retention capacity in freshwater wetlands. Sci. 228:1424–1427.

Richardson C.J., Walbridge M.R., and A. Burns. 1988. Soil chemistry and phosphorus retention capacity of North Carolina coastal plain swamps receiving sewage effluent. (Report No. 241). Water Resources Research Institute of the University of North Carolina, Raleigh, NC.

SAS Institiute. 1999. SAS Version 8.2. SAS Inst., Cary, NC.

Sallade, Y.E., and J.T. Sims. 1997. Phosphorus transformations in the sediments of Delaware's agricultural drainageways: II. Effect of reducing conditions on phosphorus release. J. Environ. Qual. 26:1579-1588.

Schwertmann, U. and R.M. Cornell. 1991. Iron Oxides in the Laboratory: Preparation and Characterization. VCH Publishing,Weinheim, Germany.

Schwertmann, U., Friedl, J., Stanjek, H., and D.G. Schulze. 2000. The effect of Al on Fe oxides. XIX. Formation of Al-substituted hematite from ferrihydrite at 25ºC and pH 4 to 7. Clays and Clay Minerals. 48:159-172.

Segal, R.G., and R.M. Sellers. 1984. Redox reactions at solid-liquid interfaces. pp. 97-129 In: A.G. Sykes (Ed.) Advances in Inorganic and Bioinorganic Mechanisms, vol. 3. Academic Press, London.

Sharpley, A.N., T.C. Daniel, and D.R. Edwards. 1993. Phosphorus movement in the landscape. J. Prod. Agric. 6, no. 4:492-500.

Sibanda, H.M., and S.D. Young. 1986. Competitive adsorption of humus acids and phosphate on goethite, gibbsite and two tropical soils. J. Soil Sci. 37:197-204.

Sims, J.T., R.R. Simard, and B.C. Joern. 1998. Phosphorus loss in agricultural drainage: Historical perspectives and current research. J. Environ. Qual. 27:277-293.

Sivasanker, S. 2002. Catalyst Deactivation. pp. 253-263. InB. Viswanathan, S. Sivasanker and A.V. Ramaswamy. (ed.) Catalysis Principles and Applications. Narosa Publishing, New Delhi, India.

Sparks, D.L., 1989. Kinetics of Soil Chemical Processes. Academic Press, San Diego, CA.

Sposito. G. 1989. The chemistry of soils. Oxford University Press, New York, NY.

Stumm, W. and J.J. Morgan. 1996. Aquatic Chemistry. John Wiley & Sons, New York, NY.

Tichang Sun, Paige, C.R., and W.J. Snodgrass. 1996. The effect of cadmium on the transformation of ferrihydrite into crystalline products at pH 8. Water, Air and Soil Pollution. 91:307-325.

Vadas, P.A., and J.T. Sims. 1998. Redox status, poultry liter, and phosphorus solubility in Atlantic coastal plain soils. Soil Sci. Am. J. 62: 1025-1034.

Van Riemsdijk, W.H. and J. Lyklema. 1980. The raction of phosphate with aluminum hydroxide in relation with phosphate binding in soils. Colloids and Surfaces. 1:33-44.

Violante, A., Colombo, C. and A. Buondonno. 1991. Competitve adsorption of phosphate and oxalate by aluminum oxides. Soil Sci. Soc. Am. J. 55:65-70.

Wang, S, Johnston, C.T., Bish, D.L. White, J.L., and S.L. Hem. 2003. Water-vapor adsorption and surface area measurement of poorly crystalline boehmite. J. Coll. Interface Sci. 260:26-35.

Willet, I.R., and R.B. Cunningham. 1983. Influence of sorbed phosphate on the stability of ferric hydrous oxide under controlled pH and Eh conditions. Aust. J. Soil Res. 21:301-308.

Williams, B.G., and W.H. Patrick, Jr. 1971. Effect of Eh and pH on the dissolution of Strengite. Nature (London) Phys. Sci. 234:16-17.

Young, E.O., and D.S. Ross. 2001. Phosphate release from seasonally flooded soils: A laboratory microcosm study. J. Environ. Qual. 30:91-101.

APPENDIX FIGURES

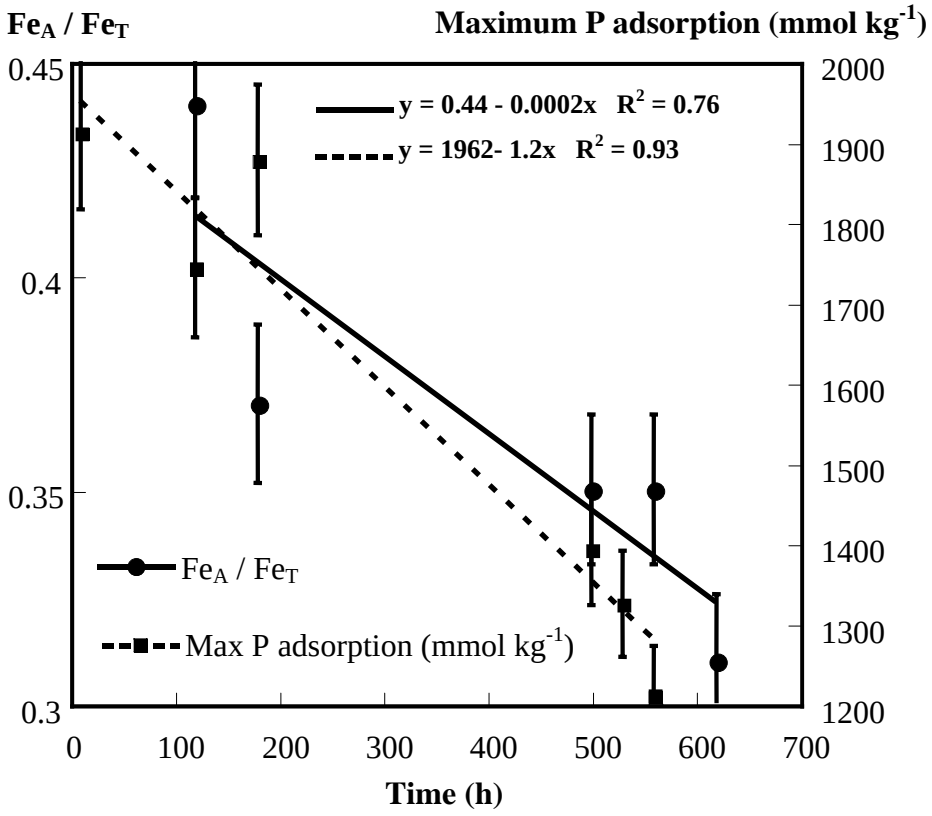

Figure A.1. Trends in the maximum P adsorption capacity and crystallinity of ferrihydrite in stock suspension as determined by periodic monitoring experiments.

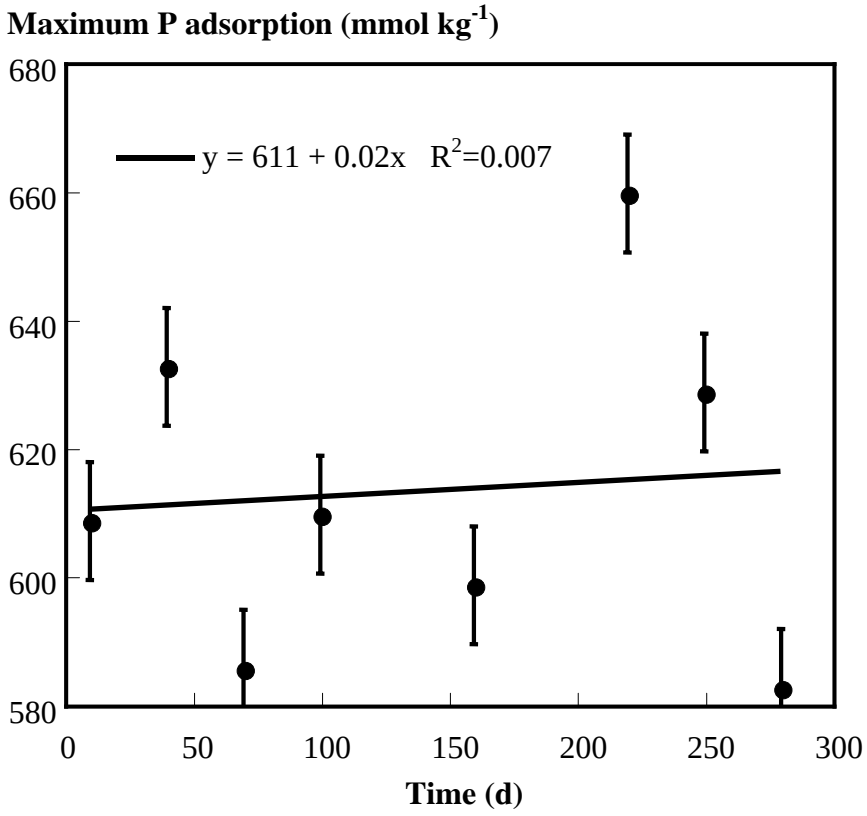

Figure A.2. Trends in the maximum P adsorption capacity during periodic monitoring of boehmite stock suspension.

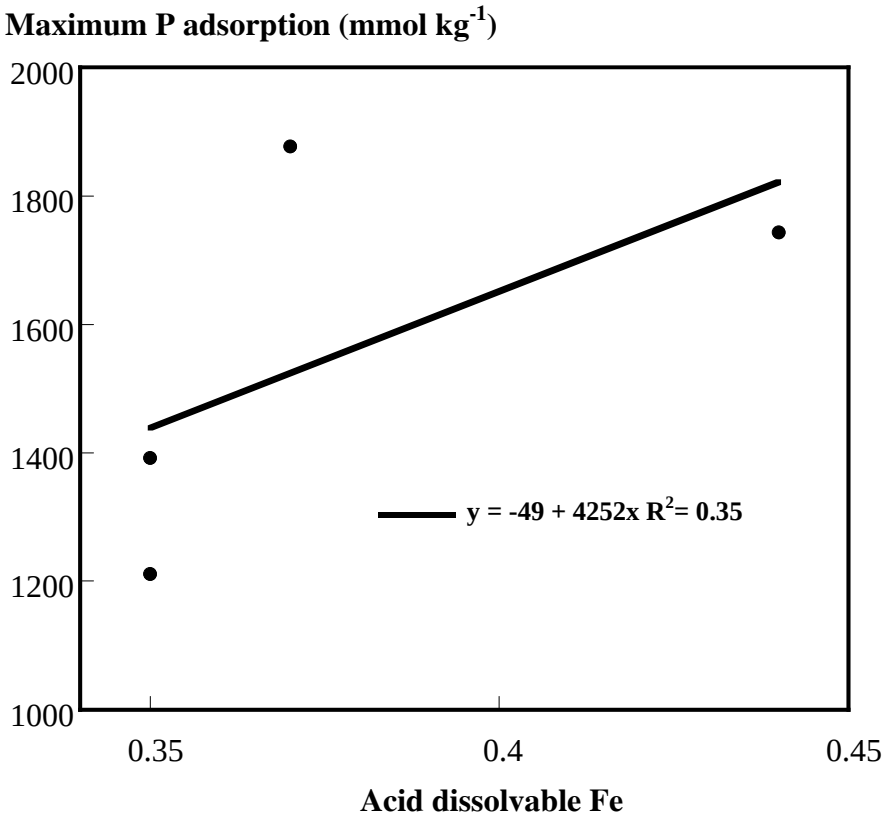

Figure A.3. Linear regression analysis of the maximum P adsorption capacity versus acid extractable Fe during periodic monitoring of ferrihydrite stock suspension.

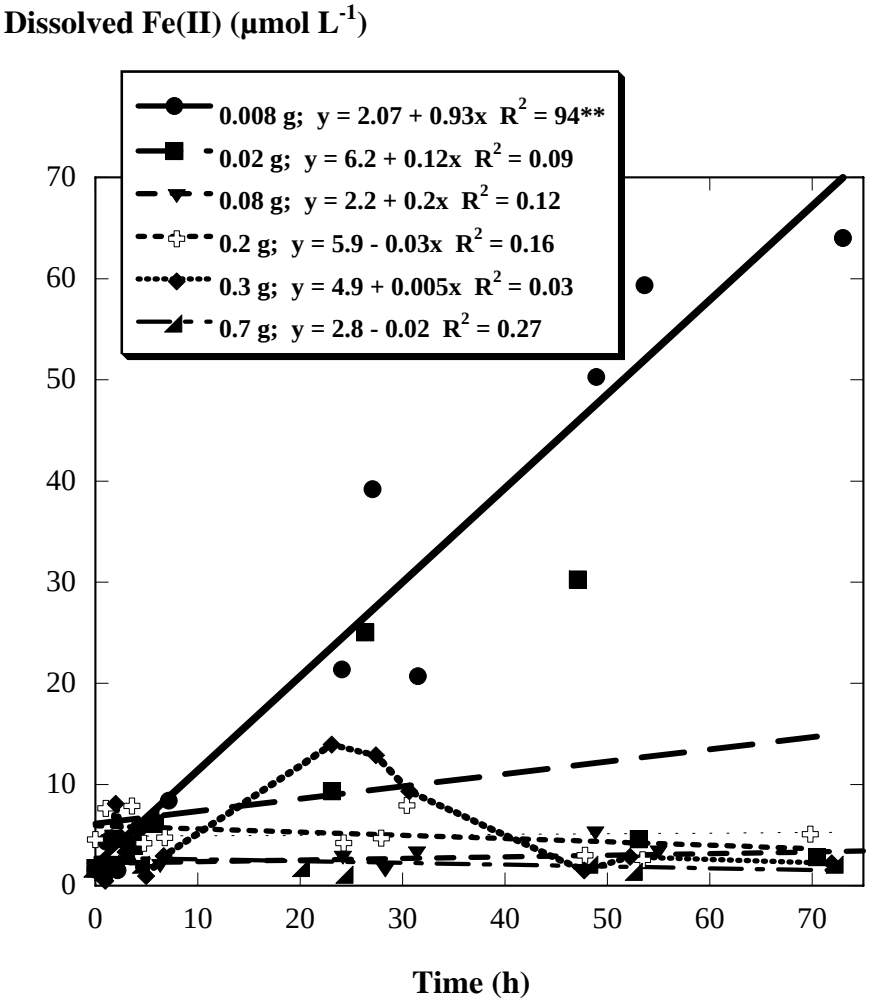

Figure A.4. Trends in dissolved Fe(II) over time for 72-h redox reactor experiments with 0.5 g ferrihydrite, 0.008 to 0.7 g boehmite, and 750 mmol P kg^{-1} solids. **$p < 0.01$

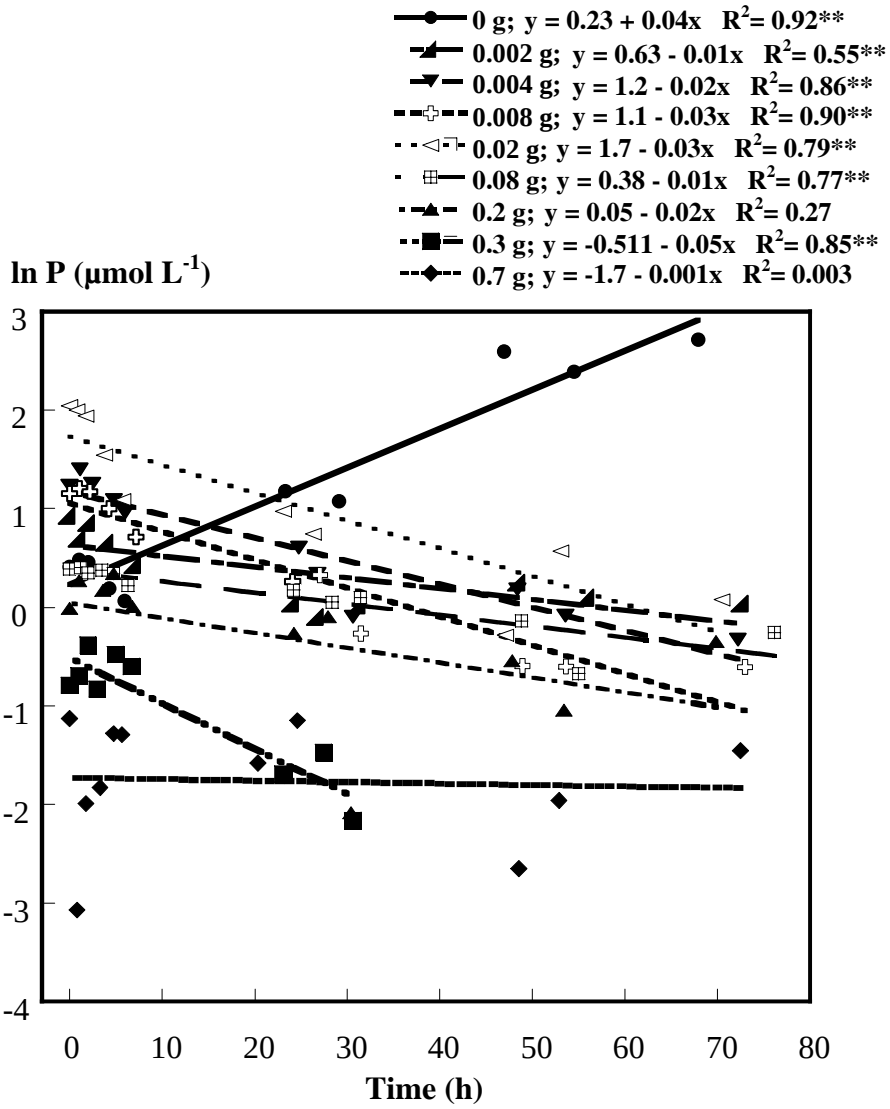

Figure A.5. First order kinetic models fit to the dissolved P data in mixed ferrihydrite/boehmite reduction reactor systems with 750 mmol P kg^{-1}.
**$p < 0.01$

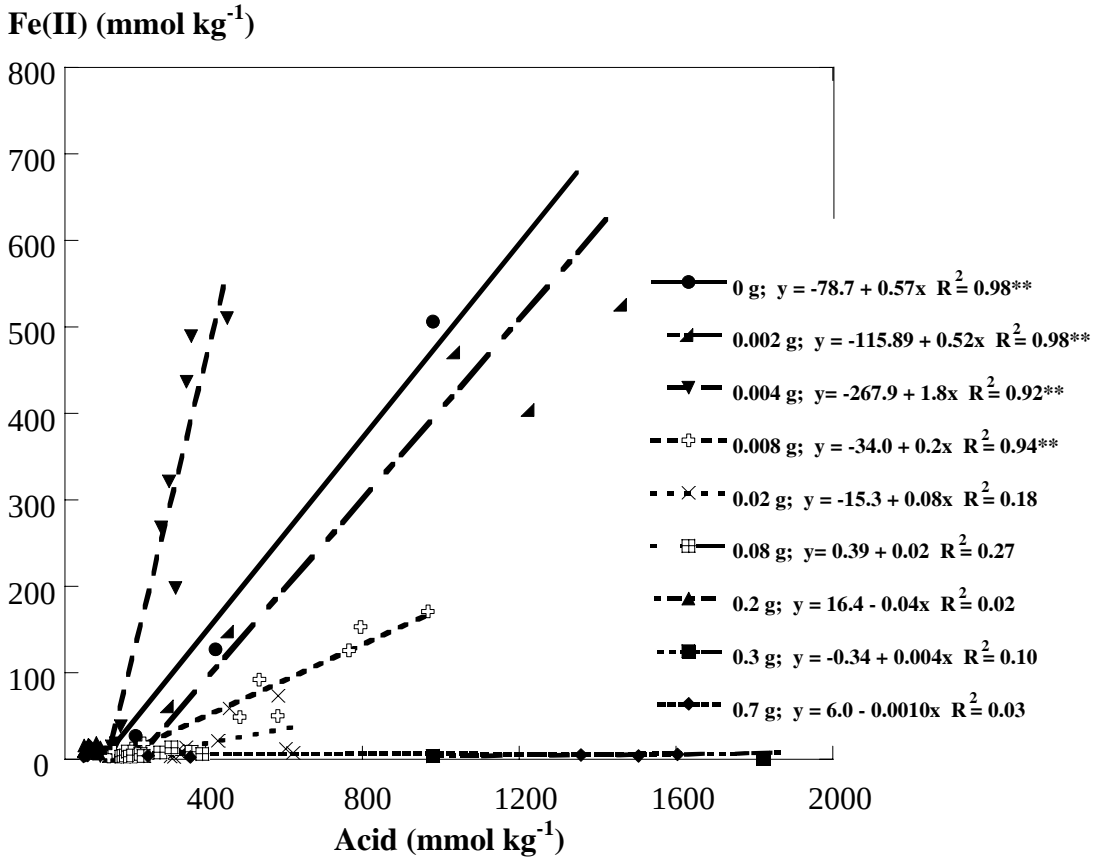

Figure A.6. Dissolved Fe(II) as a function of added acid for reduction reactor experiments with 0.5 g ferrihydrite, 0 to 0.7 g boehmite, and 750 mmol P kg^{-1}.

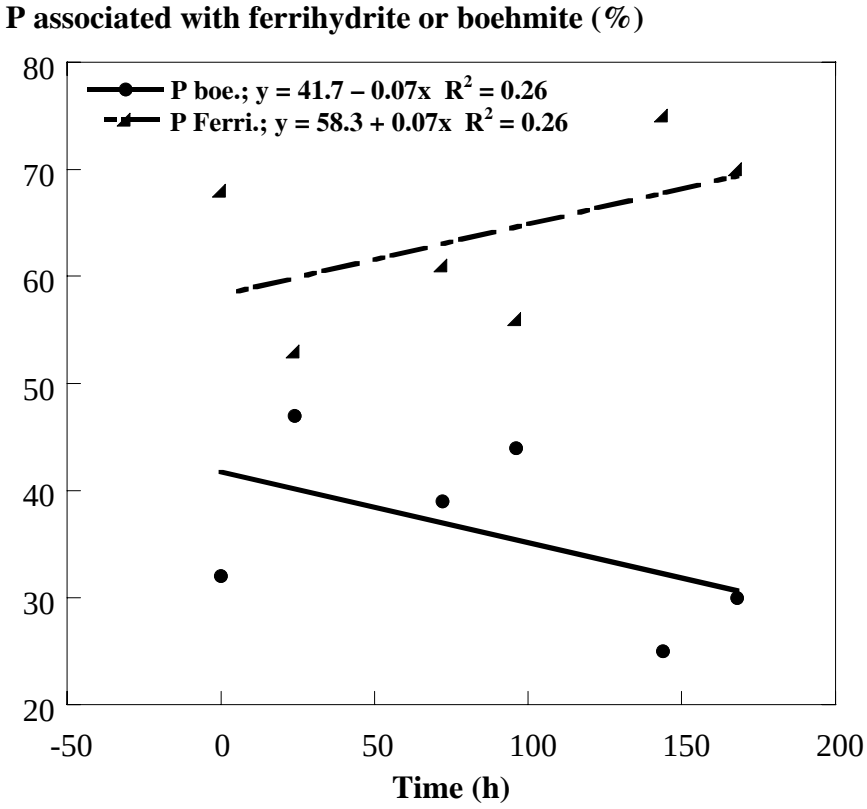

Figure A.7. Linear regression analysis for the association of P with ferrihydrite or boehmite as determined by XANES analysis for a 168 h 1:1 ferrihydrite : boehmite reduction reactor experiment with 750 mmol P kg^{-1} total solids.

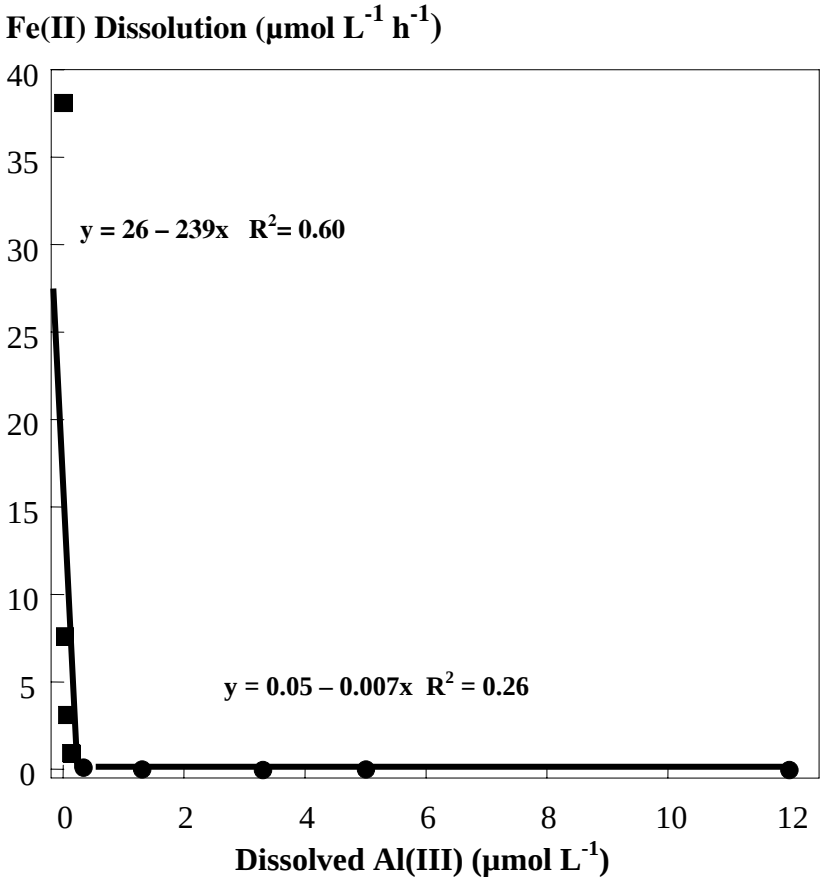

Figure A.8. Trends in Fe(II) dissolution rate as a function of dissolved Al(III) (assuming complete boehmite dissolution) for systems with 0.5 g ferrihydrite, 0 to 0.7 g boehmite, and 750 mmol P kg^{-1}.

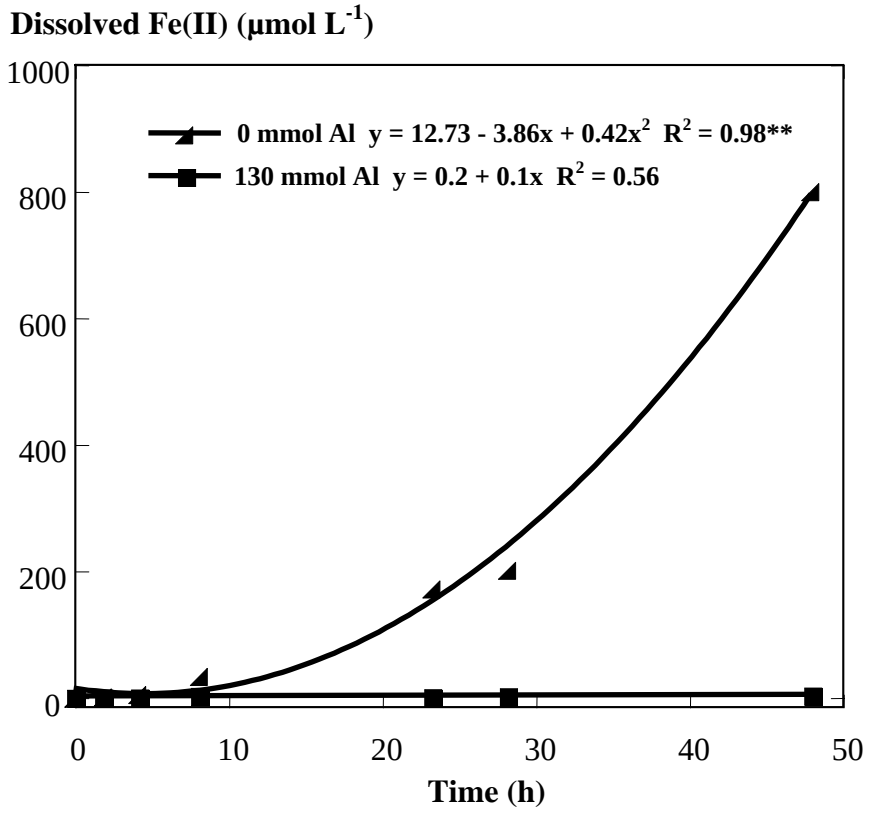

Figure A.9. Trends in dissolved Fe(II) for redox reactor systems with 0 or 130 mmol Al kg^{-1} sorbed on 10 % Pt on activated carbon catalyst. **p < 0.01